TimeSeed: Effective Time Series Forecasting with Sparse Endogenous Variables

Zhaowang Wu [1] **Kaixin Deng** [2] **Hua Yan** [1]

Abstract

Time series forecasting has long relied on dense endogenous observations, yet in many real-world scenarios, such data is scarce or even absent. Existing approaches attempt to compensate with exogenous variables, but their reliance on incomplete endogenous histories makes them brittle under data scarcity. In this work, we introduce sparse endogenous forecasting as a new setting, where exogenous sequences and only sparse endogenous observations are available. To tackle this problem, we propose TimeSeed, a lightweight architecture that redefines sparse forecasting as a context reconstruction task. By jointly exploiting the stability of exogenous sequences and the limited but informative endogenous signals, TimeSeed reconstructs robust historical representations and transforms forecasting into a tractable sequence-based prediction problem. Remarkably, TimeSeed achieves this with a purely linear architecture using only 0.19M parameters, consistently outperforming state-of-the-art deep models on seven real-world benchmarks, with an average improvement of 13.01% in MSE and 7.54% in MAE. These results establish sparse endogenous forecasting as a practical and promising paradigm, opening a new direction for time series analysis under extreme data scarcity. Code is available at this repository: https://github.com/wuzhaow/TimeSeed.

1. Introduction

Nowadays, time series forecasting has become an important tool widely applied in various domains. However, in many real-world scenarios, endogenous variables are often sparsely observed, as illustrated in Figure 1 (a), encompassing applications such as weather forecasting (Ren et al., 2021; Lin et al., 2022; Lam et al., 2023), industrial forecasting (Weron, 2014; Alfares & Nazeeruddin, 2002), and battery life prediction (Sulzer et al., 2021; Fei et al., 2021).

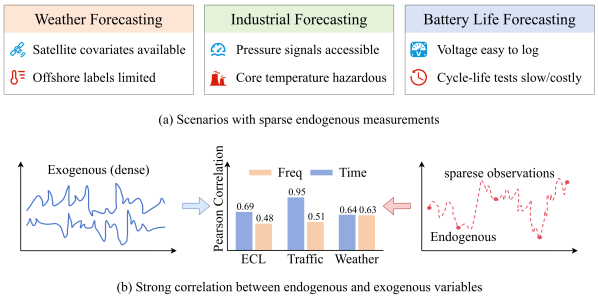

Figure 1. Scenario analysis: (a): Common real-world scenarios of sparse forecasting (b): Correlation analysis between exogenous and endogenous variables in both frequency and time domains.

Recent studies have demonstrated that incorporating the influence of *exogenous variables* (Huang et al., 2025; Pandit et al., 2023; Lu et al., 2024) can substantially enhance the predictive performance of *endogenous variables* (Motrenko et al., 2016). This enhancement is primarily attributed to the strong correlations between exogenous and endogenous variables, as illustrated in Figure 1 (b). Gradually, forecasting with exogenous variables (Gianfreda & Grossi, 2012) has emerged as a new paradigm. However, in sparse forecasting scenarios, this paradigm may become ineffective due to the absence of target information and the rigidity of the input structure.

To tackle such complex scenarios, it is essential to develop methods that leverage exogenous information and sparse endogenous observations for prediction. However, the main challenges stem from the following three aspects: **(1) Context Incompleteness:** The substantial absence of historical context for the endogenous variable leads to high uncertainty in causal discovery, especially in systems exhibiting non-stationary behavior (Moritz & Bartz-Beielstein, 2017). **(2) Unstable Dependencies:** Sparse observational data fail to reveal dependency structures within historical time series, making it difficult for models to capture trends and dynamic patterns (Liu et al., 2022b). **(3) Uncontrolled**

[1]College of Electronics and Information Engineering, Sichuan University, Chengdu, sichuan, China [2]Graduate School of Information Science and Technology, Hokkaido University, Sapporo, Hokkaido, Japan. Correspondence to: Hua Yan <yanhua@scu.edu.cn>.

Proceedings of the 43rd International Conference on Machine Learning, Seoul, South Korea. PMLR 306, 2026. Copyright 2026 by the author(s).

Anomalies: Relying on sparse endogenous observations, especially when they are outliers, may exacerbate prediction biases (Su et al., 2019).

To fill this gap, we propose TimeSeed, which reconstructs historical endogenous sequences from both endogenous and exogenous perspectives, maximally exploiting the potential of forecasting under sparse observations. Technically, we leverage the physical similarity (Huang et al., 2025; Pandit et al., 2023; Lu et al., 2024) between exogenous and endogenous variables by extracting more stable sequential features from exogenous sequences that are homogeneous to the endogenous variable. Furthermore, to further enhance reconstruction stability, we propose the Adaptive Scale Reconstructor, which constructs multi-resolution representations of sparse endogenous sequences and adaptively supplements the reconstruction of the endogenous context. By reconstructing the historical context, we transform the challenging original prediction task into a sequence-based prediction task, thereby significantly reducing the forecasting difficulty. Besides, TimeSeed is built entirely on linear layers, which greatly reduces computational cost. We conduct extensive experiments on seven real-world datasets, and the results demonstrate that the proposed model achieves outstanding performance in terms of both MAE and MSE. This demonstrates its ability to produce accurate forecasts even with limited data. The main contributions are summarized as follows:

- We propose a new prediction paradigm that relies exclusively on exogenous variables and sparse observations of the endogenous variable to forecast its future values. This effectively addresses the challenge of limited historical data for endogenous variables.
- We propose TimeSeed, a lightweight model that leverages dense exogenous and sparse endogenous sequences within a two-stage paradigm of context reconstruction and hierarchical prediction. Endogenous periodic and trend components are captured via Time Domain Aggregator and Frequency Domain Aggregator, and refined with an Adaptive Scale Reconstructor, thereby enabling more accurate forecasts.
- We conduct comprehensive experiments on seven real-world time series forecasting datasets. TimeSeed achieves an average reduction of 13.01% in MSE and 7.54% in MAE, with only 0.19M parameters, demonstrating its ability to significantly enhance forecasting accuracy in data-sparse settings while maintaining a compact architecture.

2. Related Work

2.1. Forecasting with Exogenous Variables

Exogenous variables, as key factors in improving the accuracy of endogenous variable prediction, are receiving increasing attention (Tayal et al., 2024). In traditional statistical methods, ARIMAX (Williams, 2001) has been widely used across various fields, while SARIMAX (Vagropoulos et al., 2016) further introduces radiation forecasting as an exogenous variable to enhance the accuracy of photovoltaic power generation prediction. In recent years, with the advancement of computing power and deep learning techniques, researchers have proposed various enhanced models that integrate exogenous variables. TiDE (Das et al., 2023) constructs an MLP-based encoder-decoder architecture, integrating exogenous information through feature projection and a temporal decoder. TimeXer (Wang et al., 2024b) is the first to empower the Transformer with the ability to process exogenous variables, establishing a bridge between endogenous and exogenous information through an interaction mechanism between patch-level endogenous representations and variable-level exogenous representations. In addition, NBEATSx (Olivares et al., 2023) combines neural basis functions with exogenous variables to effectively enhance power price forecasting performance. However, these models overly rely on exogenous-to-endogenous mapping, which becomes unreliable under sparse endogenous observations due to scale misalignment, leading to degraded predictive performance. Therefore, it is necessary to explore both sparse endogenous-to-endogenous and exogenous-to-endogenous perspectives to offset information loss and improve endogenous prediction accuracy.

2.2. Lightweight Forecasting

In recent years, the field of long-term time series forecasting (LTSF) (Lin et al., 2023; Zhang & Yan, 2023; Wu et al., 2022; Liu et al., 2022a; Zhou et al., 2022a; Tang & Zhang, 2025; Qiu et al., 2024) has seen a surge in lightweight models. DLinear (Zeng et al., 2023) achieves accurate forecasting using only linear layers and a decomposition strategy. CycleNet(Lin et al., 2024a) utilizes learnable parameters to simulate periodic variations across datasets, enabling plug-and-play lightweight forecasting. FITS (Xu et al., 2023) introduces a low-pass filter in the frequency domain to reduce parameter requirements, compressing the model size to approximately 10k parameters. SparseTSF(Lin et al., 2024b) decouples periodicity and trend through cross-period sparse forecasting. It first downsamples the original series using a fixed periodicity and then predicts each downsampled subsequence. MixLinear (Ma et al., 2024) further combines temporal and frequency domain feature extraction. By downsampling the series, it reduces the parameter complexity of linear models from $O(N^2)$ to $O(N)$, achieving efficient

computation. However, the above methods focus solely on lightweight modeling of the temporal characteristics of the target variable, without considering the crucial relationship between exogenous and endogenous variables (Huang et al., 2025; Das et al., 2023; Wang et al., 2024b), where a factor that is particularly important in endogenous variable prediction scenarios. Therefore, to facilitate lightweight extraction exogenous knowledge in such contexts, it is crucial to develop a compact modeling approach that captures deep correlations between endogenous and exogenous variables, enabling efficient and accurate endogenous prediction.

3. Method

3.1. Problem Settings

Unlike traditional time series prediction, we rely only on sparse endogenous series S as auxiliary information rather than full endogenous inputs. Using less endogenous variables for prediction means less information is available. Given an exogenous variable time series $X = \{x_{1:T}^{(1)}, x_{1:T}^{(2)}, ..., x_{1:T}^{(N)}\} \in \mathbb{R}^{T\times N}$ and sparse endogenous variable series $S \in \mathbb{R}^{T^{en}}$, where $x_{1:T}^{(i)}$ represents the i-th exogenous variable, T represents the length of the lookback window, $T^{en} \ll T$ indicates the length of the sparse endogenous sequence, and N represents the number of exogenous variables, the task goal is to predict the future multi-step endogenous time series $Y = \{y_{T+1}, y_{T+2}, ..., y_{T+L}\} \in \mathbb{R}^{L\times 1}$. Here, L represents the number of future time steps to predict. The overall process can be described as a function mapping: $f(X, S) \to Y$.

3.2. Structure Overview

Since the absence of endogenous variables can substantially degrade predictive performance, our motivation is to transform the inherently complex sparse forecasting task into a sequence-based prediction task by reconstructing historical endogenous sequences. This multi-stage problem decomposition approach effectively enhances the robustness of prediction. Specifically, the reconstruction leverages the intrinsic consistency between endogenous and exogenous variables by aligning with the trends (Figure 2, left) and periodic patterns (Figure 2, middle-bottom) of exogenous variables, as well as by utilizing the sparse endogenous sequence itself (Figure 2, right).

As illustrated in Figure 2 (middle-top), our proposed model accepts exogenous sequences X and sparse endogenous observations S as inputs. Following mainstream decomposition-based models (Wu et al., 2021; Wang et al., 2023; Zhou et al., 2022b), we use a moving average method, denoted as $\mathrm{Decomposition}(X; o)$, to downsample the input exogenous sequences X, yielding the separated trend component $X_t \in \mathbb{R}^{T\times N}$ and periodic component $X_s \in \mathbb{R}^{T\times N}$, where o denotes the kernel size of average pooling. For these two distinct components extracted from the exogenous sequences, we design the TDA and FDA blocks to reconstruct trend and periodic components, respectively. For the sparse endogenous observations, we propose the ASR to perform multi-scale reconstruction. Finally, the reconstruction outputs of these three modules are integrated via the Hierarchical Forecasting module to generate the final prediction results.

3.3. Time Domain Aggregator

For different variables, similar time series patterns exist within the same period. Even in cases where endogenous variables are missing, the periodic of the endogenous variable can be restored by learning the periodicity of other variables. Based on this observation, the TDA is designed to learn the periodic features of endogenous variables by leveraging exogenous variables. Specifically, for the periodic term, we first apply the patch operation to separate the features of each patch:

$$P_s^{ex} = \mathrm{Patch}(X_s, stride) \tag{1}$$

Here, $\mathrm{Patch}(\cdot)$ represents the sub-patch operation on historical exogenous variables. $P_s^{ex} \in \mathbb{R}^{P\times C\times N}$ is output of $\mathrm{Patch}(\cdot)$. C represents the length of the patch, and $P = \frac{T-C}{stride} + 1$ represents the number of patches. More detailed analysis can be found in the Appendix K.

Then we aggregate the same period of different variables. Thus, a mapping from the period of the exogenous variable to the period of the endogenous variable is established:

$$P_s^{en} = \text{Patch-Agg}(P_s^{ex}) \tag{2}$$

$\text{Patch-Agg}(\cdot)$ is implemented through a linear layer along the variable axis. $P_s^{en} \in \mathbb{R}^{C\times P}$ is the aggregated one-variable feature, which could be expressed as the reconstructed endogenous variable.

Each variable exhibits a continuous time series pattern within the same period. We obtain the future period changes of endogenous variables by aggregating the same phases in the period terms of the endogenous variables during different periods:

$$P_s^{'en} = \text{Patch-Interact}(\mathrm{Transpose}(P_s^{en})) \tag{3}$$

$\text{Patch-Interact}(\cdot)$ is implemented through a linear layer, and $P_s^{'en} \in \mathbb{R}^{C\times P}$ is the endogenous feature after patch interaction. We merge specified dimensions to obtain the output $P_s^{'en} = \mathrm{Reshape}(P_s^{'en}) \in \mathbb{R}^{T\times 1}$, which represents the period term for predicting endogenous variables.

3.4. Frequency Domain Aggregator

It is observed that different variables share similar trend patterns, and these patterns can be reconstructed by aggre-

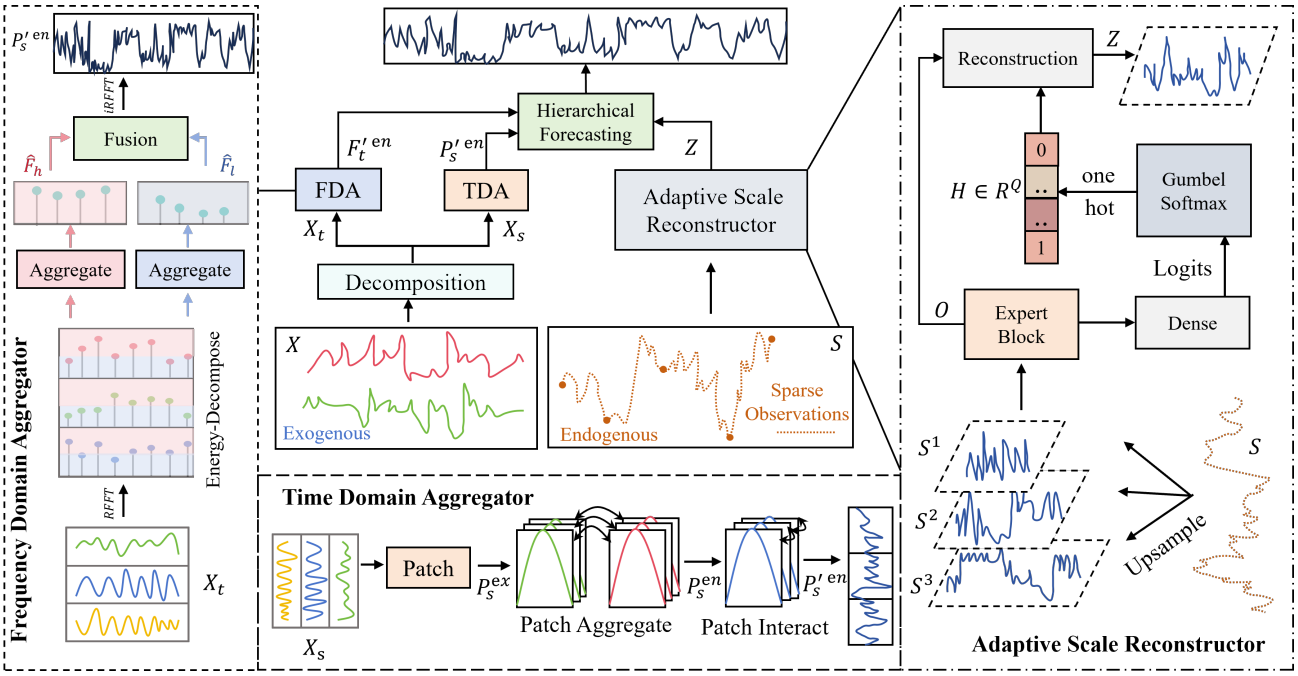

Figure 2. Overall architecture of TimeSeed, consisting of Frequency Domain Aggregator, Time Domain Aggregator, and Adaptive Scale Reconstructor, designed for sparse endogenous variables.

gating trends across variables. Since trends are usually concentrated in the low-frequency domain, directly modeling them poses the risk of either overlooking local variations or distorting the main trend. Therefore, we perform operations in the frequency domain, where dominant trend-related components and local variation-related components are more clearly separated.

Specifically, we map trend signals to the frequency domain through real Fast Fourier Transform to more directly identify the dominant trend components:

$$F_t = \mathrm{RFFT}(X_t) \tag{4}$$

Here $\mathrm{RFFT}(\cdot)$ represents real Fast Fourier Transform. $F_t \in \mathbb{R}^{(T/2+1)\times N}$ is the frequency domain representation of the trend component of the exogenous variable.

We then perform secondary decomposition on the frequency-domain signals based on their amplitude, obtaining high-energy components that correspond to dominant trends and low-energy components that correspond to local fluctuations:

$$A_t = \mathrm{Abs}(F_t) \tag{5}$$

$$F_h, F_l = \text{Energy-Decompose}(F_t, A_t, K) \tag{6}$$

Here, $\mathrm{Abs}(\cdot)$ computes the energy, and $A_t \in \mathbb{R}^{(T/2+1)\times N}$ represents the distribution of energy. $\text{Energy-Decompose}(\cdot)$ separates K high-energy and $T-K$ low-energy components according to the magnitude of the frequency amplitude by analyzing the spectrum. $F_h \in \mathbb{R}^{K\times N}$ and $F_l \in \mathbb{R}^{(T/2+1-K)\times N}$ represent the high-energy and low-energy components within the trend of the exogenous variable, respectively.

Modeling these two components separately effectively leverages local details to refine predictions, while avoiding the domination of predictions by high-energy components. Specifically, we learn the mapping relationships between the dominant trends and local details of exogenous variables , and those of endogenous variables.

$$\hat{F}_h, \hat{F}_l = \mathrm{AggHigh}(F_h), \mathrm{AggLow}(F_l) \tag{7}$$

Here, $\mathrm{AggHigh}(\cdot)$ and $\mathrm{AggLow}(\cdot)$ are both implemented through frequency domain linear layer along the variable axis. $\hat{F}_h \in \mathbb{R}^{K\times 1}$ and $\hat{F}_l \in \mathbb{R}^{(T/2+1-K)\times 1}$ represent univariate features, which can be regarded as the high-energy and low-energy components within the trend of the endogenous variable, respectively.

Finally, through the inverse real Fast Fourier Transform, we obtain the trend of the reconstructed endogenous variable:

$$F_t^{'en} = \mathrm{iRFFT}(\hat{F}_h + \hat{F}_l) \tag{8}$$

Here, iRFFT represents inverse real Fast Fourier Transform, and $F_t^{'en} \in \mathbb{R}^{T\times 1}$ represents the reconstructed trend term of the endogenous variable.

3.5. Adaptive Scale Reconstructor

In order to fully reconstruct the endogenous variables, our proposed Adaptive Scale Reconstructor generates multi-resolution sequence representations through multi-scale upsampling. The original sequence is compressed into a broader representation space, allowing the model to automatically select the most appropriate scale based on the input features.

Specifically, we construct endogenous representations cross different resolutions $q \in \{1, 2, \ldots, Q\}$:

$$S^q = \mathrm{Upsample_q}(S) \tag{9}$$

where $\mathrm{Upsample_q}(\cdot)$ denotes the q-th upsampling operation applied to the input sequence S. At the q-th layer, the output sequence length is expanded from the original T^{en} to $T^{en} \times 2^q$. This hierarchical upsampling progressively enlarges the temporal resolution, enabling the model to perform reconstructions from multiple perspectives.

$$O^q = \mathrm{ExpertBlock_q}(S^q) \tag{10}$$

where $\mathrm{ExpertBlock_q}(\cdot)$ the q-th expert module, which can be flexibly replaced with different task-specific networks, and $O^q \in \mathbb{R}^d$ represents the output of the q-th expert with d denoting the hidden dimension. Each expert learns scale-specific feature representations, thereby effectively avoiding feature entanglement across different scales.

To enable the model to adaptively select the optimal scale according to the data characteristics, we further introduce the $\mathrm{Gumbel\ Softmax}$ (Jang et al., 2016) to optimize the scale selection process:

$$H = \mathrm{Gumbel\ Softmax}(\mathrm{Dense}(\{O^1, ..., O^Q\})) \tag{11}$$

where $\mathrm{Dense}(\cdot)$ generates the corresponding logits, and $H \in \mathbb{R}^Q$ indicates the model's adaptive selection of resolution. After obtaining the most appropriate scale, the model performs feature reconstruction based on the selected representation:

$$Z = \mathrm{Reconstruction}(\{O^1, ..., O^Q\}, H) \tag{12}$$

where $\mathrm{Reconstruction}(\cdot)$ reconstructs the historical time series at the most appropriate resolution O according to the selection scheme H, and Z denotes the reconstructed sequence.

3.6. Hierarchical Forecasting

The final forecast is obtained by combining the reconstructed trend $F_t^{'en}$ and periodic components $P_s^{'en}$ (both derived from exogenous variables), with the reconstructed historical endogenous sequence Z (derived from the sparse endogenous sequence). This combined result is then passed through the model's prediction head:

$$\hat{Y}_{1:T} = F_t^{'en} + P_s^{'en} + Z \tag{13}$$

$$\hat{Y}_{T+1:T+L} = \mathrm{Prediction}(\hat{Y}_{1:T}) \tag{14}$$

Here, $\mathrm{Prediction}(\cdot)$ is implemented through a linear layer along the temporal axis, $\hat{Y}_{1:T}$ corresponds to the reconstruction of historical endogenous variables, and $\hat{Y}_{T+1:T+L}$ represents the prediction.

4. Experiments

To evaluate the performance of TimeSeed under scenarios with sparse endogenous observations, we conduct extensive experiments based on a novel time series forecasting paradigm $f(X, S) \rightarrow Y$.

Datasets We use datasets that span multiple domains, including Energy (ETT (Zhou et al., 2021), ECL (Wu et al., 2021)), Weather (Wu et al., 2021), and Traffic (Wu et al., 2021). For dataset partitioning, we follow standard protocols (Lin et al., 2024a;b). Specifically, the ETT datasets are split into training, validation, and test sets with a ratio of 6:2:2, while the remaining datasets follow a 7:1:2 split. More details are provided in the Appendix A.

Baselines We compare TimeSeed with several state-of-the-art time series forecasting models. Include: Complex Transformer-based architectures: DUET (Qiu et al., 2024), TimeXer (Wang et al., 2024b), iTransformer (Liu et al., 2023), and PatchTST (Nie et al., 2022); Lightweight MLP-based models: TimeMixer (Wang et al., 2024a), FITS (Xu et al., 2023), CycleNet (Lin et al., 2024a), FilterNet (Yi et al., 2024) [1], SparseTSF (Lin et al., 2024b), and DLinear (Zeng et al., 2023).

Implementation Details For TimeSeed, we fix the patch length P to 16, use a historical input window T of 96 time steps, and T_{en} is set to 4 by uniformly sampling the 96-step sequence at 24-step intervals. Forecasting performance is evaluated at horizons $L \in \{96, 192, 336, 720\}$. The number of high-energy components K is set to 10, the number of resolutions Q is set to 3, and $\mathrm{ExpertBlock}$ is implemented using a multi-layer perceptron. We upsample the sparse endogenous series and maintain the length of the exogenous sequences, ensuring compatibility with baseline inputs and enabling fair comparison across models. In addition, we unify the hyperparameters across all models and report the rerun results. More details are provided in the Appendix A.

[1] Implemented in TexFilter and PaiFilter, respectively

4.1. Main Results

We validate the effectiveness of TimeSeed on long-term time series forecasting tasks under sparse scenarios (sparsity ratio of 4%) across seven mainstream benchmark datasets. As shown in the experimental results in Table 1, TimeSeed achieves nearly optimal performance across all datasets. Specifically, under sparse settings, it yields an average MSE improvement of 15.04% on the ETTh1 dataset and 19.24% on the Traffic dataset, demonstrating a clear advantage over DLinear and PatchTST, which represent competitive Linear-based and Transformer-based models, respectively. Notably, as shown in the experimental results in Table 2, when endogenous variables are missing, several state-of-the-art models exhibit performance degradation, likely due to their heavy reliance on complete endogenous sequences particularly under more challenging single-point sparse forecasting scenarios. More results are provided in Appendix M and F.

4.2. Effect of Sparsity Ratios

Table 3 presents TimeSeed's performance under varying sparsity ratios. The results demonstrate that as the sparsity ratio increases (i.e., a higher proportion of endogenous variables), predictive accuracy improves consistently across both ETTh2 and ETTm2 datasets. Specifically, on the ETTh2 dataset, increasing the sparsity ratio yields a 16.5% reduction in average MSE. On the ETTm2 dataset, we observe a similar trend with an 18.8% decrease in average MSE. These performance gains are sustained across all forecasting horizons, confirming that incorporating richer endogenous information substantially enhances forecasting capability under sparse endogenous settings.

4.3. Ablation Study

To further analyze the contribution of each component to the model's performance, we performed ablation analysis on the Time Domain Aggregator, Frequency Domain Aggregator, and Adaptive Scale Reconstructor to assess their individual impacts. As shown in Table 4, we draw the following three conclusions: (1) All modules positively contribute to the performance of TimeSeed, with improvements in MSE ranging from 5.31% to 12.30%. (2) Comparatively, the contribution of high-energy information to the prediction results is slightly lower, leading to an MSE improvement of about 5.31%. (3)Based on a two-stage decomposition and forecasting paradigm, outperforms the Direct Forecasting approach in terms of evaluation metrics. Notably, on the ETTh2 and ETTm2 datasets, TimeSeed achieves average improvements of 27.4% and 14.2% in MSE and MAE, respectively. This is because the two-stage approach decouples the sequence features, allowing the reconstruction stage to focus more on capturing trends and periodic patterns, thereby enhancing robustness(4) Furthermore, different datasets rely to varying degrees on information from the time domain, the frequency domain, and the multi-resolution reconstructions derived from sparse endogenous series. More details can be found in the Appendix G.

4.4. Model Analysis

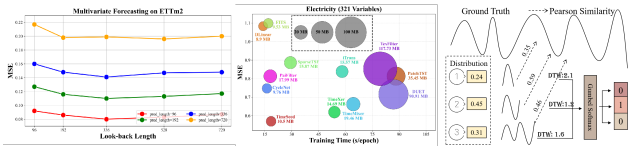

Figure 3. Analysis of the TimeSeed. Left : Performance across various prediction lengths with different look-back window sizes. Middle : Comparison of model efficiency. Right: Selection distribution of TimeSeed across multi-level sequences.

Different Look-back Window Sizes To assess robustness, we vary look-back lengths on ETTm2. Longer windows provide richer history but may cause redundancy for linear models. As shown in Figure 3 (Left), TimeSeed benefits from longer windows, with clear MSE gains at horizons 192 and 336, demonstrating stable performance across input lengths. Detailed results are in Appendix B.

Efficiency Analysis To assess computational efficiency, we compared TimeSeed with 11 state-of-the-art models on GPU memory and training time. Under the same settings of hidden dimension 128 and batch size 1, results in Figure 3 (Middle) demonstrate that TimeSeed achieves superior performance in both memory efficiency and predictive accuracy. It consumes only 10.5MB of memory, approximately 71.5% of TimeXer's 14.69MB. In addition, its training time is roughly 30% of that of TimeXer, emphasizing its computational efficiency. More results are in the Appendix C.

Case Study To validate the effectiveness of the adaptive multi-resolution selection mechanism in the proposed ASR, we analyze a representative case from the ETTh1 dataset. As shown in Figure 3 (Right), we further report the correlation and Dynamic Time Warping between the reconstructed sequences at each resolution and the ground truth. The second resolution exhibits the highest correlation with the ground truth, achieving a Pearson coefficient of 0.59 and a DTW of 1.2, which indicates its superiority as the most appropriate resolution. Furthermore, ASR accurately identifies this candidate sequence, thereby validating the effectiveness of its adaptive multi-resolution selection mechanism.

4.5. Sensitivity Analysis

Different Data Scale To further explore the potential of TimeSeed under sparse settings, we design three more challenging forecasting scenarios: sparser endogenous series, fewer exogenous variables, and shorter historical exogenous series. As shown in Figure 4 (left), the performance of Time-

Table 1. Unified hyperparameter for long-term time series forecasting results are **based on sparse endogenous variable setting**, with a 24-hour sampling interval.

Model	TimeSeed		DUET		iTrans		DLinear		TimeXer		TimeMixer		PatchTST		FITS		CycleNet		TexFilter		PaiFilter		SparseTSF	
Metric	MSE	MAE	MSE	MAE	MSE	MAE	MSE	MAE	MSE	MAE	MSE	MAE	MSE	MAE	MSE	MAE	MSE	MAE	MSE	MAE	MSE	MAE	MSE	MAE
ETTh1	**0.096**	**0.242**	0.159	0.311	0.186	0.345	0.113	0.262	0.444	0.569	0.162	0.309	0.228	0.381	0.142	0.297	0.116	0.261	0.144	0.294	0.152	0.306	0.158	0.316
ETTh2	**0.272**	**0.410**	0.381	0.491	0.902	0.811	0.409	0.493	0.342	0.465	0.274	0.412	0.574	0.617	0.553	0.587	0.291	0.423	0.328	0.456	0.475	0.545	0.622	0.635
ETTm1	**0.068**	**0.194**	0.157	0.303	0.143	0.282	0.075	0.205	0.344	0.499	0.141	0.305	0.104	0.245	0.079	0.216	0.104	0.246	0.145	0.294	0.109	0.254	0.499	0.466
ETTm2	**0.149**	**0.289**	0.284	0.417	0.373	0.495	0.165	0.303	0.266	0.404	0.179	0.325	0.208	0.362	0.202	0.343	0.157	0.296	0.176	0.318	0.176	0.320	0.193	0.339
Weather	**0.002**	**0.034**	0.006	0.058	0.011	0.080	0.009	0.066	0.827	0.789	0.394	0.552	0.004	0.050	0.007	0.067	0.003	0.039	0.005	0.052	0.012	0.077	0.007	0.068
ECL	**0.529**	**0.558**	0.641	0.618	0.749	0.676	0.832	0.699	0.575	0.573	1.674	0.987	0.714	0.659	1.087	0.817	0.822	0.690	0.775	0.677	1.027	0.809	0.709	0.656
Traffic	**0.403**	**0.433**	0.574	0.561	0.483	0.493	0.584	0.542	1.396	1.028	1.251	0.828	0.499	0.509	0.790	0.672	0.876	0.678	0.584	0.548	0.703	0.619	1.276	0.886

Table 2. Unified hyperparameter for long-term time series forecasting results are **based on a single endogenous variable setting**, with the point selection strategy choosing the most recent time step.

Model	TimeSeed		DUET		iTrans		DLinear		TimeXer		TimeMixer		PatchTST		FITS		CycleNet		TexFilter		PaiFilter		SparseTSF	
Metric	MSE	MAE	MSE	MAE	MSE	MAE	MSE	MAE	MSE	MAE	MSE	MAE	MSE	MAE	MSE	MAE	MSE	MAE	MSE	MAE	MSE	MAE	MSE	MAE
ETTh1	**0.101**	**0.249**	0.189	0.332	0.179	0.332	0.116	0.268	0.380	0.525	0.538	0.632	0.168	0.321	0.123	0.278	0.343	0.492	0.125	0.276	0.121	0.273	0.168	0.328
ETTh2	**0.269**	**0.409**	0.367	0.481	0.912	0.816	0.296	0.430	0.344	0.466	0.540	0.576	0.621	0.648	0.723	0.680	0.343	0.465	0.400	0.499	0.462	0.537	0.676	0.661
ETTm1	**0.061**	**0.189**	0.096	0.237	0.083	0.223	0.065	0.196	0.325	0.489	0.488	0.566	0.080	0.218	**0.061**	0.190	0.233	0.400	0.073	0.206	0.083	0.222	0.090	0.231
ETTm2	**0.176**	**0.321**	0.283	0.417	0.345	0.468	0.206	0.347	0.268	0.401	0.239	0.377	0.200	0.345	0.248	0.424	0.283	0.415	0.216	0.356	0.231	0.377	0.249	0.392
ECL	**0.569**	**0.580**	0.715	0.659	0.838	0.716	1.083	0.799	0.619	0.594	0.662	0.628	0.813	0.701	1.099	0.812	0.747	0.657	0.853	0.708	0.813	0.699	0.886	0.734
Traffic	0.482	**0.489**	0.585	0.570	0.505	0.507	0.602	0.553	1.549	1.078	1.405	1.041	**0.477**	0.498	0.916	0.741	1.555	1.083	0.763	0.646	1.027	0.805	1.597	0.990
Weather	**0.002**	**0.034**	0.006	0.059	0.009	0.073	0.009	0.074	0.742	0.737	2.527	1.406	0.004	0.048	0.007	0.065	0.833	0.789	0.005	0.056	0.012	0.078	0.005	0.059

Table 3. Forecasting performance on ETTh2 and ETTm2 under different sparsity ratios of endogenous to exogenous features (4%–50%). SR denotes sparsity ratios (endogenous : exogenous).

SR		4% (default)		8%		16%		25%		33%		50%	
Metric		MSE	MAE	MSE	MAE	MSE	MAE	MSE	MAE	MSE	MAE	MSE	MAE
ETTh2	96	0.186	0.336	0.167	0.318	0.154	0.304	0.152	0.303	0.147	0.297	**0.144**	**0.293**
	192	0.234	0.379	0.212	0.361	0.204	0.352	0.195	0.343	0.198	0.347	**0.189**	**0.337**
	336	0.288	0.426	0.267	0.410	0.265	0.409	0.250	0.396	0.249	0.396	**0.241**	**0.389**
	720	0.380	0.499	0.374	0.495	0.364	0.489	0.350	0.480	0.344	0.476	**0.334**	**0.470**
	AVG	0.272	0.410	0.255	0.396	0.247	0.388	0.237	0.381	0.234	0.379	**0.227**	**0.372**
ETTm2	96	0.092	0.224	0.075	0.202	0.071	0.197	0.070	0.194	0.070	0.195	**0.070**	**0.194**
	192	0.127	0.269	0.109	0.249	0.103	0.240	0.102	0.239	**0.102**	**0.238**	0.103	0.239
	336	0.160	0.304	0.139	0.283	0.135	0.278	0.132	0.275	0.131	0.274	**0.131**	**0.274**
	720	0.217	0.360	0.192	0.337	0.183	0.327	0.184	0.328	0.183	0.327	**0.182**	**0.325**
	AVG	0.149	0.289	0.129	0.268	0.123	0.261	0.122	0.259	0.122	0.259	**0.121**	**0.258**

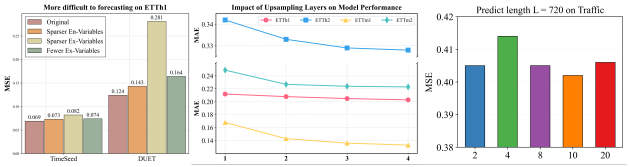

Figure 4. Sensitivity Analysis to different Data Scales, Resolutions and High-energy Components.

Seed decreases by 5.80%, 18.84%, and 7.25% compared to the original setting under the three different configurations. In contrast, DUET shows a larger decline, with decreases of 15.32%, 126.61%, and 32.26%, respectively. It is evident that among these three factors, the length of the historical exogenous series has the greatest impact on forecasting performance. TimeSeed consistently maintains the best predictive performance across all cases.

Different Resolution To further investigate the impact of ASR under different resolution choices, we vary the number of upsampling layers from 1 to 4. As shown in Figure 4 (middle), with more upsampling layers, the number of available resolutions increases. On the ETT datasets, performance improves progressively, with a particularly significant gain when increasing the layer count from 1 to 2. Consider-

Table 4. Ablation study results. FDA denotes Frequency Domain Aggregator, ASR denotes Adaptive Scale Reconstructor and TDA denotes Time Domain Aggregator.

Datasets	ETTh1		ETTm1		ETTh2		ETTm2	
Metric	MSE	MAE	MSE	MAE	MSE	MAE	MSE	MAE
TimeSeed	**0.096**	**0.242**	**0.068**	**0.194**	**0.272**	**0.410**	**0.149**	**0.289**
w/o Agghigh (Eq. 7)	0.112	0.242	0.084	0.215	0.284	0.420	0.155	0.295
w/o Agglow (Eq. 7)	0.110	0.257	0.077	0.206	0.285	0.420	0.159	0.299
w/o Patch-Interact (Eq. 3)	0.119	0.265	0.074	0.202	0.291	0.424	0.156	0.298
w/o FDA	0.118	0.265	0.088	0.222	0.299	0.432	0.154	0.293
w/o TDA	0.117	0.263	0.083	0.219	0.376	0.488	0.154	0.295
w/o ASR	0.099	0.246	0.082	0.218	0.279	0.415	0.176	0.322
Direct Forecasting	0.124	0.274	0.074	0.204	0.400	0.493	0.160	0.300

ing both performance and efficiency, we set the number of resolutions Q to 3.

Different High-energy Components As shown in Figure 4 (Right), increasing the decomposition factor initially improves performance; however, beyond a certain point (e.g., 8), the gains plateau or even diminish. This phenomenon suggests that an appropriately chosen number of high-energy components is beneficial for model performance. Therefore, we unify $K = 10$ in our implementation for experiments. More detailed results can be found in the Appendix E.

4.6. Reliability Analysis of Reconstruction

Frequency-domain Reconstruction Figure 5 (a) shows that the reconstructed and true trend components on ETTh1. It is clearly observable that the two curves almost completely overlap. This indicates that TimeSeed can accurately reconstruct endogenous trends from exogenous inputs, effectively capturing the relationship between exogenous and endogenous trends and validating the effectiveness of our frequency domain multi-granularity modeling. More results are in Appendix D.

Time-domain Visualization Figure 5 (b) shows weight heatmaps of the Time Domain Aggregator. The left panel corresponds to the implementation of $\text{Patch-Agg}(\cdot)$, and the right panel to $\text{Patch-Interact}(\cdot)$. The repeated horizontal purple stripes on the left indicate that $\text{Patch-Agg}(\cdot)$ is sensitive to periodic features in the input sequence. In contrast, the heatmap on the right exhibits a smooth top-down gradient, suggesting that $\text{Patch-Interact}(\cdot)$ effectively captures cross-period feature correlations. These distributions suggest the model adaptively emphasizes phase-aligned information, enhancing temporal structure modeling.

Reconstruction Correlation In Figure 5 (right), we report the Pearson correlation coefficients between the reconstructed endogenous periodic and trend components obtained by TDA and FDA and the corresponding ground truth. Overall, both TDA and FDA achieve sufficiently high reconstruction fidelity, with average correlations of 0.532 and

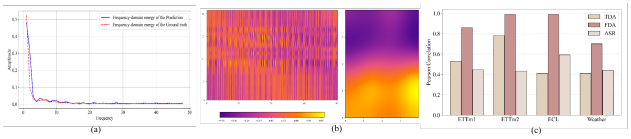

Figure 5. Reliability analysis of reconstruction. (a) Frequency spectrum of the reconstructed trend component of historical endogenous variables. (b) Visualization of the weights in the TDA. (c) Correlation between reconstruction the ground truth.

0.885, respectively. This further highlights the effectiveness of our two-stage decomposition and forecasting paradigm based on reconstruction.

4.7. More Experiments

Real-world Benchmark: We have incorporated the real clinical dataset $PhysioNet$. As shown in Table 5, TimeSeed still achieves the best or highly competitive performance under these genuinely sparse conditions, demonstrating the robustness and practical applicability of our method. More details on the dataset are provided in the Appendix A.

Imputation + forecasting: We first use PatchTST to impute the sparse endogenous series, and then apply another state-of-the-art forecasting model (PatchTST or TimeXer) to predict future values. As shown in Table 6, TimeSeed outperforms both combinations on most datasets. On average, relative to PatchTST/PatchTST, TimeSeed reduces MSE and MAE by about 36% and 24%, and relative to PatchTST/TimeXer, by about 26% and 30%, respectively. These gains stem from the two-stage paradigm, which decouples sequence features and enables the reconstruction stage to more effectively capture trends and periodicity, improving robustness. The limited benefit of the imputation model likely results from the extreme sparsity of the endogenous observations, while adding another imputation module increases parameter count and thus the risk of overfitting.

Table 6. Comparison with the imputation–forecasting pipeline

Model	TimeSeed		PatchT/PatchT		PatchT/TimeX	
Metric	MSE	MAE	MSE	MAE	MSE	MAE
ETTh1	**0.096**	**0.242**	0.153	0.322	0.388	0.498
ETTh2	**0.272**	**0.410**	0.502	0.561	0.281	0.412
ETTm1	0.068	**0.194**	**0.041**	0.196	0.283	0.428
ETTm2	**0.149**	**0.289**	0.154	0.293	0.197	0.336

5. Conclusion

We propose TimeSeed, a novel prediction architecture tailored for scenarios with sparse endogenous variables. From both the endogenous and exogenous perspectives, TimeSeed can robustly reconstruct historical endogenous sequences by uncovering the periodic and trend-related re-

Table 5. Results on the sparse real-world PhysioNet dataset

Model	TimeSeed		DUET		DLinear		TimeXer		FilterNet		SparseTSF	
Metric	MSE	MAE	MSE	MAE	MSE	MAE	MSE	MAE	MSE	MAE	MSE	MAE
PhysioNet	**0.30**	**0.24**	0.34	**0.24**	0.33	**0.24**	0.78	0.53	0.33	**0.24**	0.35	0.25

lationships between exogenous and endogenous variables. Moreover, it leverages ASR to supplement the reconstructed endogenous information with signals from the sparse endogenous sequences. All experimental results show that TimeSeed achieves the best performance across all benchmarks, demonstrating its ability to deliver high-accuracy predictions even under extreme data scarcity. Furthermore, thanks to its linear-based architecture, TimeSeed exhibits excellent computational efficiency. These advantages provide a practical and effective solution to the challenge of missing data in real-world applications. In future work, we plan to explore more advanced prediction methods for more complex scenarios, such as when *endogenous variables are entirely missing*.

Impact Statement

This paper presents work whose goal is to advance the field of Machine Learning. There are many potential societal consequences of our work, none which we feel must be specifically highlighted here.

References

Alfares, H. K. and Nazeeruddin, M. Electric load forecasting: literature survey and classification of methods. *International journal of systems science*, 33(1):23–34, 2002.

Das, A., Kong, W., Leach, A., Mathur, S., Sen, R., and Yu, R. Long-term forecasting with tide: Time-series dense encoder. *arXiv preprint arXiv:2304.08424*, 2023.

Fei, Z., Yang, F., Tsui, K.-L., Li, L., and Zhang, Z. Early prediction of battery lifetime via a machine learning based framework. *Energy*, 225:120205, 2021.

Gianfreda, A. and Grossi, L. Forecasting italian electricity zonal prices with exogenous variables. *Energy Economics*, 34(6):2228–2239, 2012.

Huang, Q., Zhou, Z., Yang, K., and Wang, Y. Exploiting language power for time series forecasting with exogenous variables. In *Proceedings of the ACM on Web Conference 2025*, pp. 4043–4052, 2025.

Jang, E., Gu, S., and Poole, B. Categorical reparameterization with gumbel-softmax. *arXiv preprint arXiv:1611.01144*, 2016.

Kingma, D. P. and Ba, J. Adam: A method for stochastic optimization. *arXiv preprint arXiv:1412.6980*, 2014.

Lam, R., Sanchez-Gonzalez, A., Willson, M., Wirnsberger, P., Fortunato, M., Alet, F., Ravuri, S., Ewalds, T., Eaton-Rosen, Z., Hu, W., et al. Learning skillful medium-range global weather forecasting. *Science*, 382(6677):1416–1421, 2023.

Lin, H., Gao, Z., Xu, Y., Wu, L., Li, L., and Li, S. Z. Conditional local convolution for spatio-temporal meteorological forecasting. In *Proceedings of the AAAI conference on artificial intelligence*, volume 36, pp. 7470–7478, 2022.

Lin, S., Lin, W., Wu, W., Zhao, F., Mo, R., and Zhang, H. Segrnn: Segment recurrent neural network for long-term time series forecasting. *arXiv preprint arXiv:2308.11200*, 2023.

Lin, S., Lin, W., Hu, X., Wu, W., Mo, R., and Zhong, H. Cyclenet: enhancing time series forecasting through modeling periodic patterns. *Advances in Neural Information Processing Systems*, 37:106315–106345, 2024a.

Lin, S., Lin, W., Wu, W., Chen, H., and Yang, J. Sparsetsf: Modeling long-term time series forecasting with 1k parameters. *arXiv preprint arXiv:2405.00946*, 2024b.

Liu, M., Zeng, A., Chen, M., Xu, Z., Lai, Q., Ma, L., and Xu, Q. Scinet: Time series modeling and forecasting with sample convolution and interaction. *Advances in Neural Information Processing Systems*, 35:5816–5828, 2022a.

Liu, Y., Wu, H., Wang, J., and Long, M. Non-stationary transformers: Exploring the stationarity in time series forecasting. *Advances in neural information processing systems*, 35:9881–9893, 2022b.

Liu, Y., Hu, T., Zhang, H., Wu, H., Wang, S., Ma, L., and Long, M. itransformer: Inverted transformers are effective for time series forecasting. *arXiv preprint arXiv:2310.06625*, 2023.

Lu, J., Han, X., Sun, Y., and Yang, S. Cats: Enhancing multivariate time series forecasting by constructing auxiliary time series as exogenous variables. *arXiv preprint arXiv:2403.01673*, 2024.

Ma, A., Luo, D., and Sha, M. Mixlinear: Extreme low resource multivariate time series forecasting with 0.1 k parameters. *arXiv preprint arXiv:2410.02081*, 2024.

Moritz, S. and Bartz-Beielstein, T. imputets: time series missing value imputation in r. 2017.

Motrenko, A., Rudakov, K., and Strijov, V. Combining endogenous and exogenous variables in a special case of non-parametric time series forecasting model. *Moscow University Computational Mathematics and Cybernetics*, 40(2):71–78, 2016.

Nie, Y., Nguyen, N. H., Sinthong, P., and Kalagnanam, J. A time series is worth 64 words: Long-term forecasting with transformers. *arXiv preprint arXiv:2211.14730*, 2022.

Olivares, K. G., Challu, C., Marcjasz, G., Weron, R., and Dubrawski, A. Neural basis expansion analysis with exogenous variables: Forecasting electricity prices with nbeatsx. *International Journal of Forecasting*, 39(2):884–900, 2023.

Pandit, P., Sagar, A., Ghose, B., Dey, P., Paul, M., Alqadhi, S., Mallick, J., Almohamad, H., and Abdo, H. G. Hybrid time series models with exogenous variable for improved yield forecasting of major rabi crops in india. *Scientific Reports*, 13(1):22240, 2023.

Paszke, A. Pytorch: An imperative style, high-performance deep learning library. *arXiv preprint arXiv:1912.01703*, 2019.

Qiu, X., Wu, X., Lin, Y., Guo, C., Hu, J., and Yang, B. Duet: Dual clustering enhanced multivariate time series forecasting. *arXiv preprint arXiv:2412.10859*, 2024.

Ren, X., Li, X., Ren, K., Song, J., Xu, Z., Deng, K., and Wang, X. Deep learning-based weather prediction: a survey. *Big Data Research*, 23:100178, 2021.

Su, Y., Zhao, Y., Niu, C., Liu, R., Sun, W., and Pei, D. Robust anomaly detection for multivariate time series through stochastic recurrent neural network. In *Proceedings of the 25th ACM SIGKDD international conference on knowledge discovery & data mining*, pp. 2828–2837, 2019.

Sulzer, V., Mohtat, P., Aitio, A., Lee, S., Yeh, Y. T., Steinbacher, F., Khan, M. U., Lee, J. W., Siegel, J. B., Stefanopoulou, A. G., et al. The challenge and opportunity of battery lifetime prediction from field data. *Joule*, 5(8): 1934–1955, 2021.

Tang, P. and Zhang, W. Unlocking the power of patch: Patch-based mlp for long-term time series forecasting. In *Proceedings of the AAAI Conference on Artificial Intelligence*, volume 39, pp. 12640–12648, 2025.

Tayal, K., Renganathan, A., Jia, X., Kumar, V., and Lu, D. Exotst: Exogenous-aware temporal sequence transformer for time series prediction. *arXiv preprint arXiv:2410.12184*, 2024.

Vagropoulos, S. I., Chouliaras, G., Kardakos, E. G., Simoglou, C. K., and Bakirtzis, A. G. Comparison of sarimax, sarima, modified sarima and ann-based models for short-term pv generation forecasting. In *2016 IEEE international energy conference (ENERGYCON)*, pp. 1–6. IEEE, 2016.

Wang, H., Peng, J., Huang, F., Wang, J., Chen, J., and Xiao, Y. Micn: Multi-scale local and global context modeling for long-term series forecasting. In *The eleventh international conference on learning representations*, 2023.

Wang, S., Wu, H., Shi, X., Hu, T., Luo, H., Ma, L., Zhang, J. Y., and Zhou, J. Timemixer: Decomposable multi-scale mixing for time series forecasting. *arXiv preprint arXiv:2405.14616*, 2024a.

Wang, Y., Wu, H., Dong, J., Qin, G., Zhang, H., Liu, Y., Qiu, Y., Wang, J., and Long, M. Timexer: Empowering transformers for time series forecasting with exogenous variables. *arXiv preprint arXiv:2402.19072*, 2024b.

Weron, R. Electricity price forecasting: A review of the state-of-the-art with a look into the future. *International journal of forecasting*, 30(4):1030–1081, 2014.

Williams, B. M. Multivariate vehicular traffic flow prediction: evaluation of arimax modeling. *Transportation Research Record*, 1776(1):194–200, 2001.

Wu, H., Xu, J., Wang, J., and Long, M. Autoformer: Decomposition transformers with auto-correlation for long-term series forecasting. *Advances in neural information processing systems*, 34:22419–22430, 2021.

Wu, H., Hu, T., Liu, Y., Zhou, H., Wang, J., and Long, M. Timesnet: Temporal 2d-variation modeling for general time series analysis. *arXiv preprint arXiv:2210.02186*, 2022.

Xu, Z., Zeng, A., and Xu, Q. Fits: Modeling time series with $10k$ parameters. *arXiv preprint arXiv:2307.03756*, 2023.

Yi, K., Fei, J., Zhang, Q., He, H., Hao, S., Lian, D., and Fan, W. Filternet: Harnessing frequency filters for time series forecasting. *Advances in Neural Information Processing Systems*, 37:55115–55140, 2024.

Zeng, A., Chen, M., Zhang, L., and Xu, Q. Are transformers effective for time series forecasting? In *Proceedings of the AAAI conference on artificial intelligence*, volume 37, pp. 11121–11128, 2023.

Zhang, Y. and Yan, J. Crossformer: Transformer utilizing cross-dimension dependency for multivariate time series forecasting. In *The eleventh international conference on learning representations*, 2023.

Zhou, H., Zhang, S., Peng, J., Zhang, S., Li, J., Xiong, H., and Zhang, W. Informer: Beyond efficient transformer for long sequence time-series forecasting. In *Proceedings of the AAAI conference on artificial intelligence*, volume 35, pp. 11106–11115, 2021.

Zhou, T., Ma, Z., Wen, Q., Sun, L., Yao, T., Yin, W., Jin, R., et al. Film: Frequency improved legendre memory model for long-term time series forecasting. *Advances in neural information processing systems*, 35:12677–12690, 2022a.

Zhou, T., Ma, Z., Wen, Q., Wang, X., Sun, L., and Jin, R. Fedformer: Frequency enhanced decomposed transformer for long-term series forecasting. In *International conference on machine learning*, pp. 27268–27286. PMLR, 2022b.

A. Implementation Details

DataSets We evaluated the performance of TimeSeed on seven widely used datasets. These include the Traffic (Wu et al., 2021), Weather (Wu et al., 2021), Electricity (Wu et al., 2021), and the ETT dataset (Zhou et al., 2021). Specifically, Traffic records traffic flow freeway system of the San Francisco area, collected at hourly intervals via inductive loop detectors installed on roadways, and has been collected since 2015. Weather collects 21 weather metrics from the National Weather Service (NWS), including temperature, humidity, wind speed, and barometric pressure, covering nearly 400 weather stations across the United States. This data is collected every 10 minutes. Electricity records hourly power consumption data for 321 customers. The ETT contains electrical load and oil temperature data from two substations, which are organized into four sub-datasets: ETTh1, ETTh2, ETTm1, and ETTm2, where "h" stands for hourly sampling intervals and "m" stands for 15-minute sampling intervals. For the ETT dataset, the time period spanning from July 2016 to July 2018 includes electrical load, oil temperature, and six other relevant metrics. Overall, the datasets we use cover diverse domains such as transportation, meteorology, energy, etc., with varying temporal granularities. Detailed information about these datasets is provided in Table 7.

Real-world Benchmark: We consider the PhysioNet dataset, in which physiological variables naturally exhibit sparsity. Reliably obtainable signals such as heart rate (HR), respiratory rate (RespRate), temperature (Temp), systolic blood pressure (SysABP), diastolic blood pressure (DiasABP), and mean arterial pressure (MAP) are treated as exogenous variables, while the more sparsely measured glucose level serves as the endogenous variable. The first 24 hours of observations are used to forecast the subsequent 24 hours.

Table 7. Comparison of dataset characteristics, including key information such as the definitions of endogenous (En.Explanation) and exogenous (Ex.Explanation), prediction horizon, sampling frequency, and dataset size (training, validation, and test sets).

Dataset	ETTh1	ETTh2	ETTm1	ETTm2	ECL	Traffic	Weather
Ex.Explanation	Energy Load	Energy Load	Energy Load	Energy Load	Power consumption	Road Occupancy	Weather Indicators
En.Explanation	Oil Temperature	Oil Temperature	Oil Temperature	Oil Temperature	Power consumption	Road Occupancy	CO2-Concentration
Predict Length	(96,192,336,720)	(96,192,336,720)	(96,192,336,720)	(96,192,336,720)	(96,192,336,720)	(96,192,336,720)	(96,192,336,720)
Ex.Count	6	6	6	6	320	861	20
Sampling Frequency	1 Hour	1 Hour	15 Minutes	15 Minutes	1 Hour	1 Hour	10 Minutes
Dataset Size	(8449,2785,2785)	(8449,2785,2785)	(34369,11425,11425)	(34369,11425,11425)	(15591,5167,5165)	(110335,3415,3415)	(31426,10445,10445)

Unified Hyperparameter Settings Under our newly proposed forecasting paradigm, we fix the hyperparameters for all models and adopt the same optimization strategy to ensure fair and reproducible experiments. The detailed settings are shown in Table 8. All the experiments are implemented in PyTorch (Paszke, 2019) and conducted on a single NVIDIA 2080Ti 10GB GPU.

Table 8. Unified hyperparameter settings for all experiments. All models are optimized using the ADAM optimizer (Kingma & Ba, 2014). K the number of high-energy components corresponding to those extracted by the FDA. D_{model} represents the hidden dimension of the baseline model, and D_{ff} is the baseline model's dimension of the hidden layer in the feed-forward layer.

Dataset / Configurations	Model Hyper-parameter			Training Process				
	K	D_{model}	D_{ff}	Batchsize	Lr	Epoch	Early_stop	Loss
ETTh1	10	128	512	128	0.001	10	3	MSE
ETTh2	10	128	512	128	0.001	10	3	MSE
ETTm1	10	128	512	128	0.001	10	3	MSE
ETTm2	10	128	512	128	0.001	10	3	MSE
ECL	10	128	512	4	0.001	10	3	MSE
Traffic	10	128	512	4	0.001	10	3	MSE
Weather	10	128	512	64	0.001	10	3	MSE

B. Full Results of Different Look-back Window Size

Figure 6 and 7 presents the impact of varying look-back window sizes on the prediction accuracy of TimeSeed across the ETT series datasets.

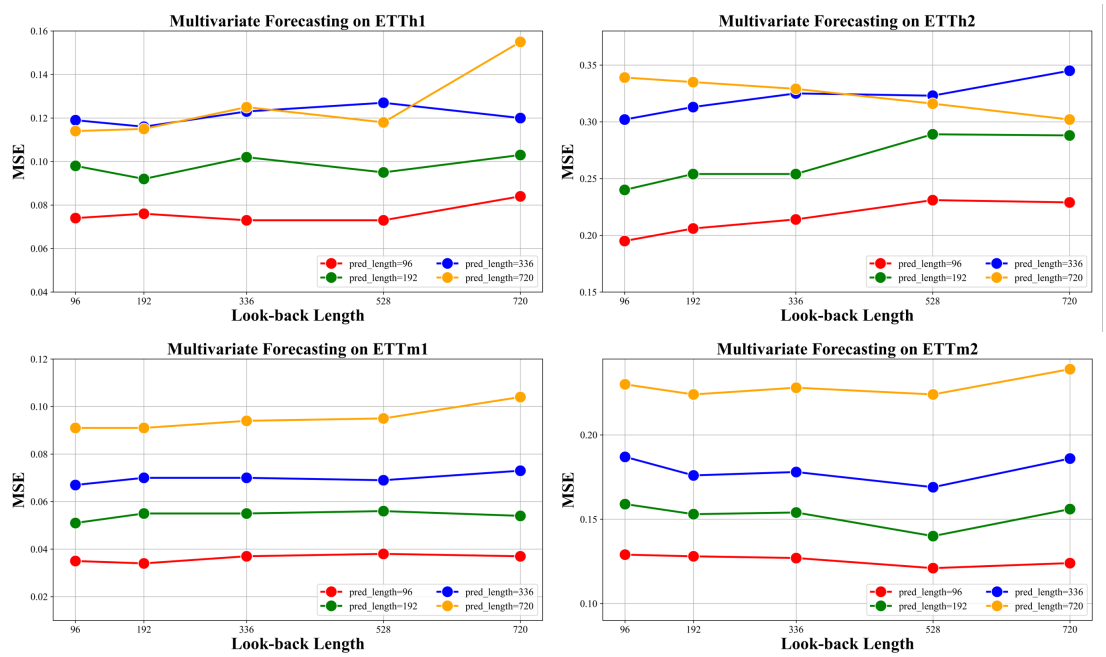

Figure 6. Performance across various prediction lengths with different look-back window sizes $T = \{96, 192, 336, 528, 720\}$ under a single endogenous setting. Each colored curve represents the performance of a specific look-back window.

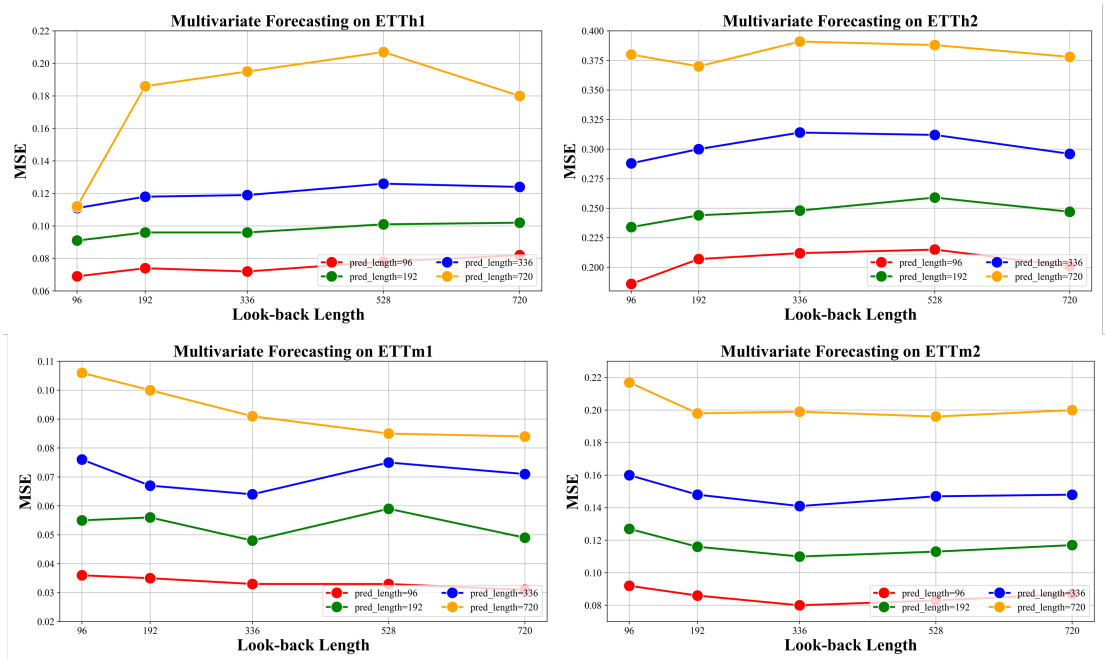

Figure 7. Performance across various prediction lengths with different look-back window sizes $T = \{96, 192, 336, 528, 720\}$ under sparse endogenous setting. Each colored curve represents the performance of a specific look-back window.

C. Full Results of Runtime Efficiency Analysis

We report the runtime efficiency of all models across all datasets in terms of training time (s/epoch) and GPU memory usage, along with predictive performance measured by MSE. As shown in Figure 8, TimeSeed fully unleashes the potential of linear layers, achieving accurate predictions while maintaining a lightweight design.

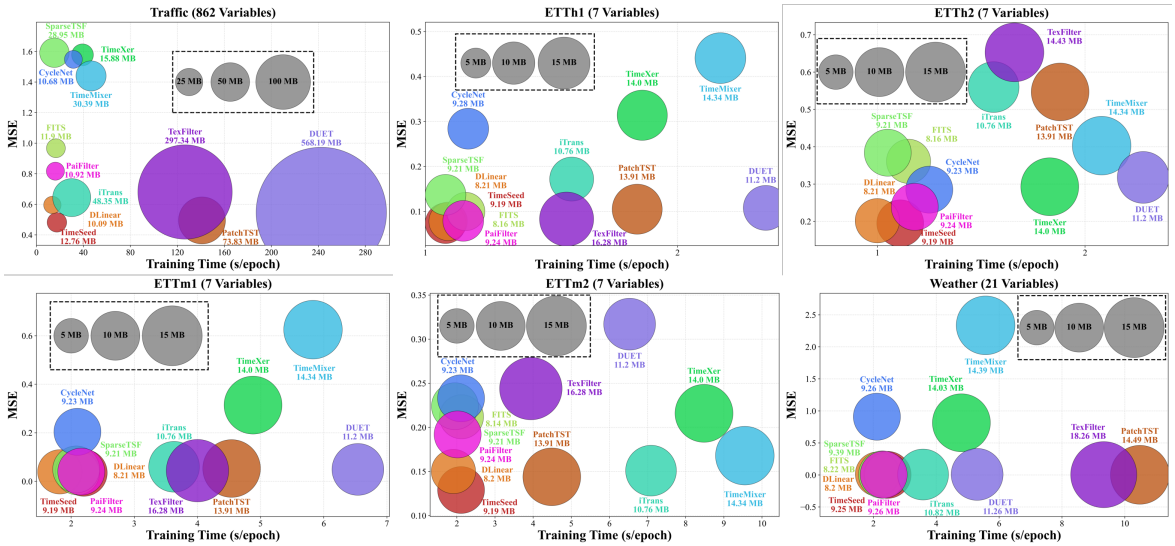

Figure 8. Comparison of model efficiency in the input-96-predict-96 setting.

D. Full Results of Frequency-domain Analysis

To further evaluate the ability of the Frequency-Domain Aggregator (FDA) to reconstruct the trend component of historical endogenous variables, we provide additional prediction cases in Figure 9. The results demonstrate that Frequency-domain Aggregator effectively leverages the trend-related information in exogenous variables and establishes robust correlations between the trends of exogenous variables and those of historical endogenous variables, thereby enabling effective reconstruction of the target trend components.

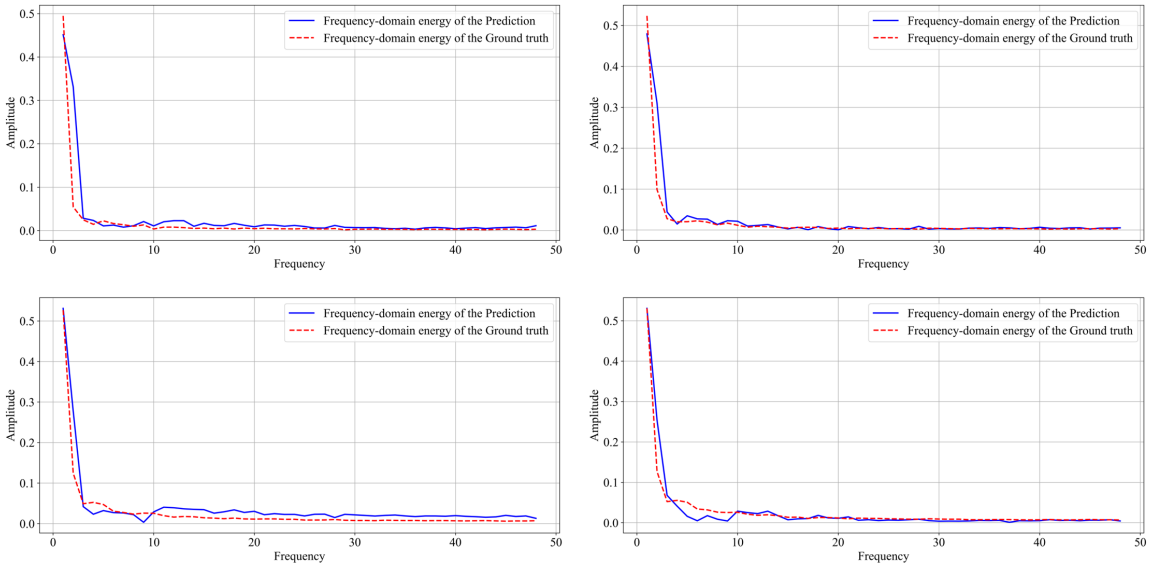

Figure 9. Frequency spectrum of the reconstructed trend component of historical endogenous variables (blue) and the ground truth (red) in the frequency domain. The closer the two curves, the better the reconstruction performance.

E. Full Results of Hyperparameter Sensitivity Analysis

In the frequency-domain decomposition module, we further split the input trend component based on an energy-oriented perspective. To explore how different decomposition thresholds affect model performance, we report the complete results of varying K values on the ECL and Traffic datasets in Figures 10, 11, 12 and 13. It is evident that the choice of decomposition threshold, reflected by different values of K, has a considerable impact on model performance. Overall, on both the ECL and Traffic datasets, as K increases, the error metrics first decrease and then gradually stabilize, with a slight rise in some cases. This indicates that excessively small thresholds fail to adequately capture the energy characteristics of the input sequence, whereas overly large thresholds may introduce redundant decomposition components, thereby impairing the model's generalization ability. The best performance is generally observed at moderate K values, suggesting that an appropriate threshold strikes a balance between preserving dominant trends and retaining local variations. In summary, the predictive performance across different K values does not vary drastically, further demonstrating the robustness of the TimeSeed.

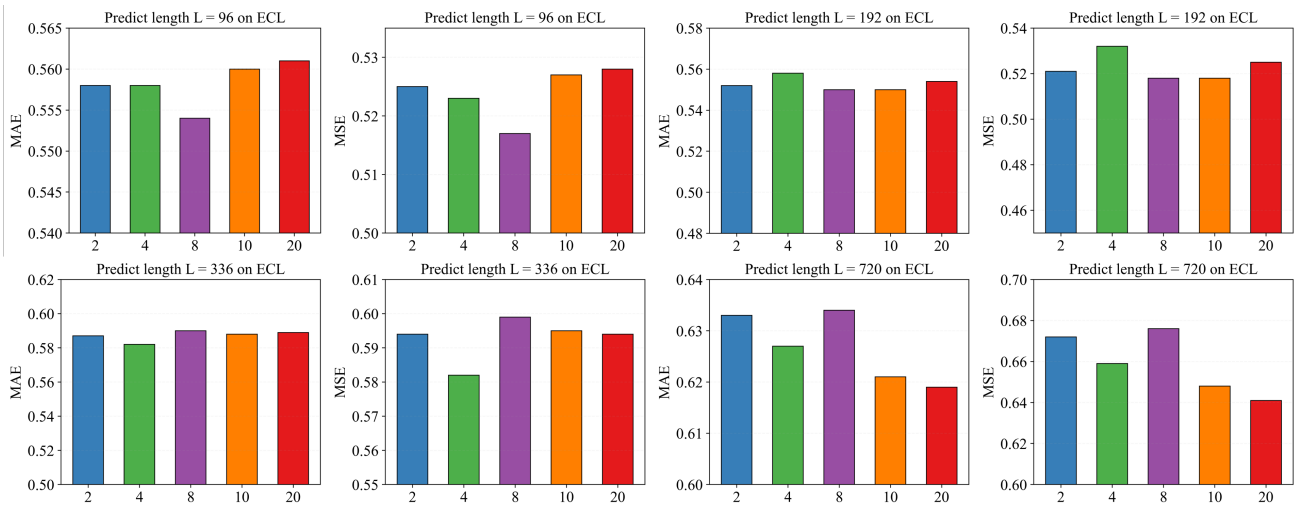

Figure 10. Impact of different K values in Energy-Decompose within the Frequency Domain Aggregator, evaluated on the ECL dataset with various prediction lengths {96, 192, 336, 720} based on a single endogenous setting.

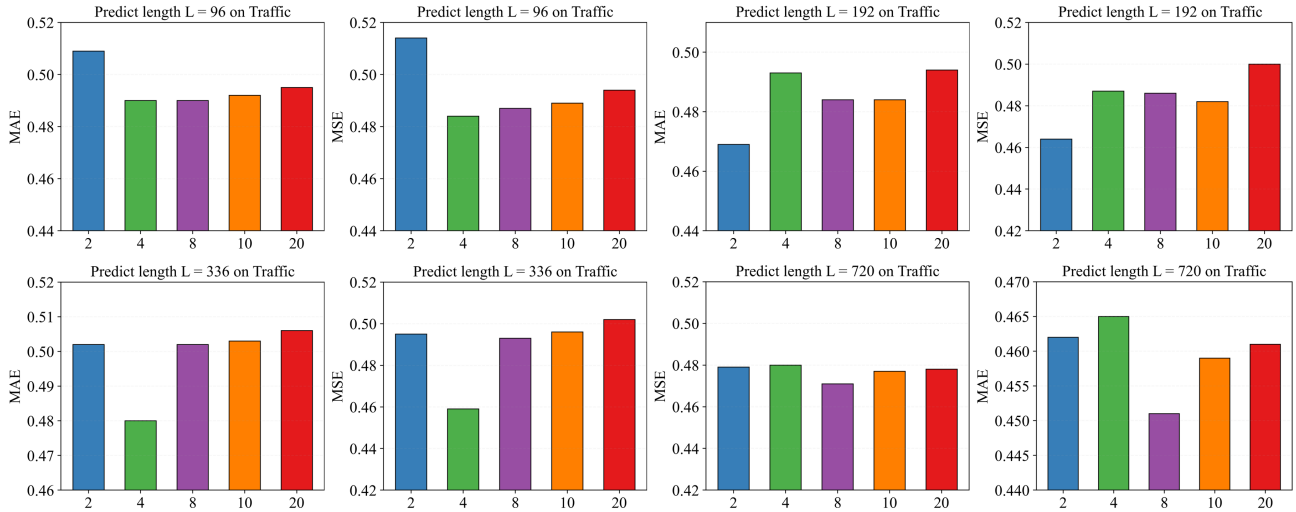

Figure 11. Impact of different K values in Energy-Decompose within the Frequency Domain Aggregator, evaluated on the Traffic dataset with various prediction lengths {96, 192, 336, 720} based on a single endogenous setting.

We evaluate the sensitivity of TimeSeed across different average pooling kernel sizes (o) and high-energy component

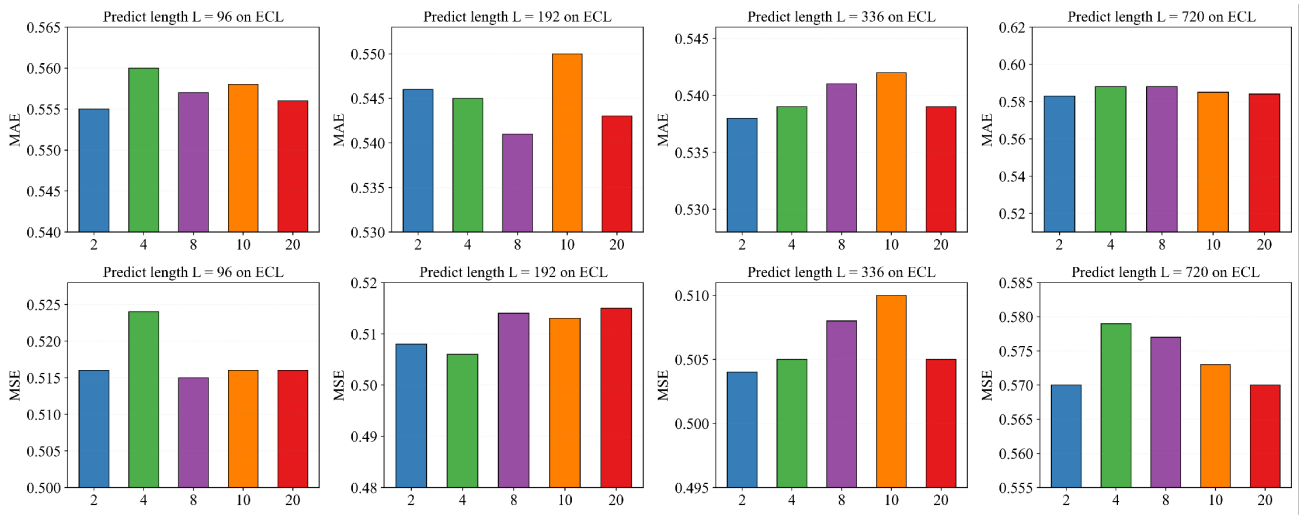

Figure 12. Impact of different K values in Energy-Decompose within the Frequency Domain Aggregator, evaluated on the ECL dataset with various prediction lengths {96, 192, 336, 720} based on sparse endogenous variable setting.

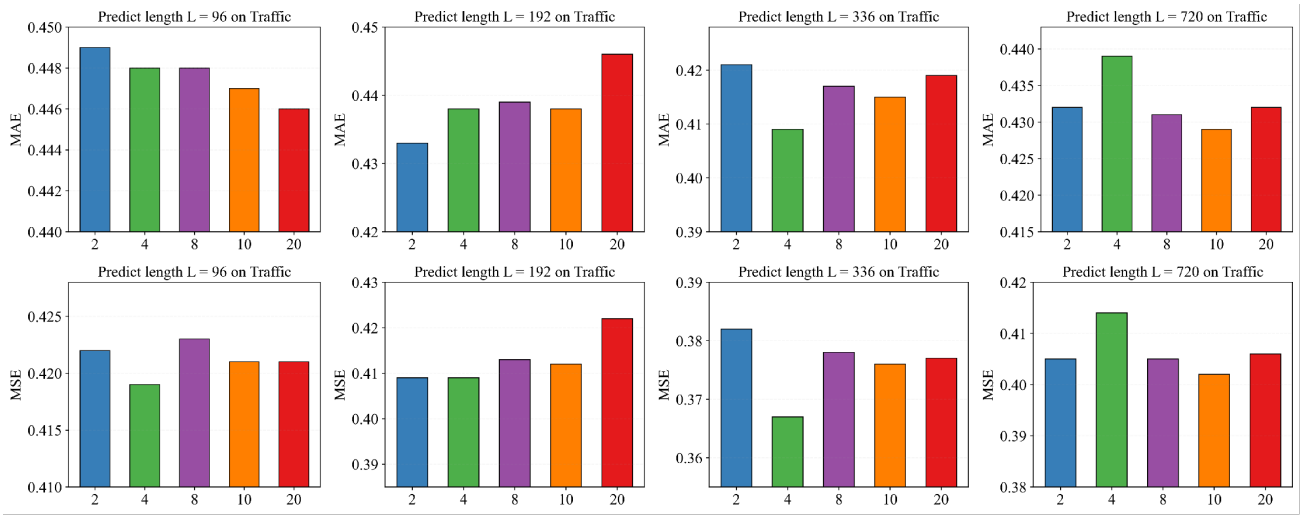

Figure 13. Impact of different K values in Energy-Decompose within the Frequency Domain Aggregator, evaluated on the Traffic dataset with various prediction lengths {96, 192, 336, 720} based on sparse endogenous variable setting.

numbers (K). As shown in Figure 14, we investigate the impact of different downsampling kernel sizes (o) on the forecasting performance of TimeSeed across various prediction lengths. The results indicate that as the value of o increases, the model performance tends to stabilize or improve. This trend is particularly evident on the Traffic and ECL datasets. In contrast, the ETTh2 dataset exhibits relatively consistent performance regardless of kernel size variations. We also observe that the most effective kernel sizes often align with the data's inherent daily, weekly, or monthly periodicities. Based on these findings, we fix the downsampling kernel size to $o = 25$ for all subsequent experiments.

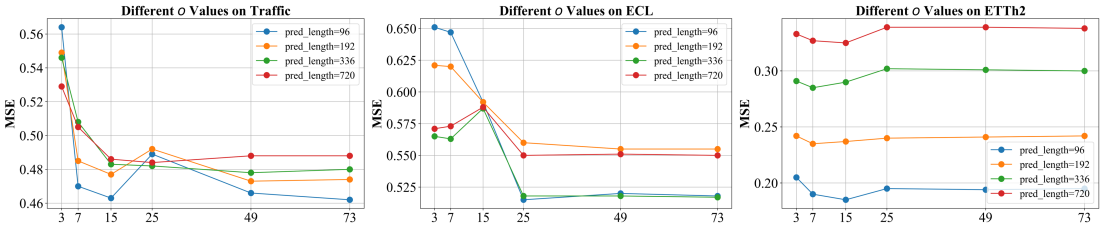

Figure 14. Performance of dfferent downsampling kernels in the Decompose module for long-term time series forecasting on Traffic, ECL and ETTh2 with input-96-predict-96 setting.

F. Full Result of Randomly Sampling Endogenous Variable

Table 9 reports the complete prediction results of TimeSeed, DLinear, TimeXer, and FITS under the strategy based on randomly sampling and uniform interval sampling. Random sampling is closer to real-world forecasting scenarios, and the comparison between the two sampling strategies reflects the impact of different sampling schemes on model performance. The results demonstrate that random sampling consistently yields inferior results relative to uniform interval sampling across most datasets, with this performance gap widening as forecasting horizons extend. This may be attributed to the fact that maintaining uniform temporal structure is more conducive to reconstructing complete historical endogenous sequences, whereas the uncertainty introduced by random sampling can reduce the model's generalization ability. Notably, across both sampling strategies and all forecasting horizons, TimeSeed consistently outperforms the baseline methods, demonstrating its robustness and effectiveness even in challenging sparse scenarios.

Table 9. Full results of unified hyperparameter for long-term time series forecasting results are based on sparse endogenous setting, with the point selection strategy randomly choosing a time step. The look-back window length is fixed at 96. The reported results represent the average performance across different forecasting horizons $L = \{96, 192, 336, 720\}$. * indicates the use of a random sampling strategy. Lower MSE and MAE values indicate better forecasting performance.

Model		TimeSeed		TimeSeed*		DLinear		DLinear*		TimeXer		TimeXer*		FITS		FITS*	
Metric		MSE	MAE	MSE	MAE	MSE	MAE	MSE	MAE	MSE	MAE	MSE	MAE	MSE	MAE	MSE	MAE
ETTh1	96	**0.069**	**0.203**	0.074	0.209	0.079	0.218	0.081	0.219	0.438	0.572	0.513	0.625	0.089	0.230	0.089	0.230
	192	**0.091**	**0.236**	0.100	0.241	0.105	0.251	0.106	0.251	0.442	0.565	0.413	0.540	0.211	0.372	0.211	0.372
	336	**0.111**	**0.262**	0.121	0.269	0.138	0.292	0.138	0.292	0.429	0.552	0.537	0.635	0.120	0.273	0.120	0.273
	720	**0.112**	**0.265**	0.189	0.350	0.131	0.288	0.130	0.288	0.464	0.588	0.643	0.715	0.149	0.311	0.148	0.310
	AVG	**0.096**	**0.242**	0.121	0.267	0.113	0.262	0.114	0.263	0.444	0.569	0.527	0.629	0.142	0.297	0.142	0.296
ETTh2	96	**0.186**	**0.336**	0.192	0.342	0.201	0.350	0.201	0.350	0.289	0.423	0.284	0.418	0.303	0.431	0.326	0.446
	192	**0.234**	**0.379**	0.234	0.380	0.255	0.397	0.252	0.396	0.330	0.457	0.325	0.455	0.333	0.460	0.355	0.475
	336	**0.288**	**0.426**	0.289	0.427	0.306	0.440	0.307	0.441	0.358	0.479	0.356	0.478	0.496	0.571	0.507	0.578
	720	**0.380**	**0.499**	0.397	0.510	0.873	0.786	0.848	0.769	0.390	0.501	0.389	0.500	1.079	0.887	1.076	0.882
	AVG	**0.272**	**0.410**	0.278	0.415	0.409	0.493	0.402	0.489	0.342	0.465	0.339	0.463	0.553	0.587	0.566	0.595
ETTm1	96	**0.036**	**0.143**	0.038	0.148	0.043	0.157	0.047	0.166	0.290	0.468	0.292	0.472	0.051	0.175	0.051	0.175
	192	**0.055**	**0.179**	0.058	0.183	0.064	0.191	0.066	0.193	0.301	0.468	0.329	0.490	0.083	0.226	0.082	0.223
	336	**0.076**	**0.210**	0.077	0.211	0.083	0.218	0.085	0.222	0.359	0.508	0.333	0.491	0.092	0.231	0.096	0.236
	720	0.106	0.246	0.105	0.244	0.111	0.253	0.115	0.258	0.426	0.551	0.451	0.563	**0.088**	0.232	0.088	**0.229**
	AVG	**0.068**	**0.194**	0.070	0.196	0.075	0.205	0.078	0.210	0.344	0.499	0.351	0.504	0.079	0.216	0.079	0.216
ETTm2	96	**0.092**	**0.224**	0.119	0.260	0.093	0.224	0.132	0.272	0.239	0.377	0.228	0.365	0.118	0.260	0.192	0.338
	192	**0.127**	**0.269**	0.151	0.297	0.135	0.276	0.164	0.309	0.245	0.384	0.259	0.395	0.151	0.298	0.201	0.346
	336	**0.160**	**0.304**	0.182	0.327	0.171	0.315	0.198	0.342	0.261	0.404	0.283	0.417	0.212	0.357	0.250	0.388
	720	**0.217**	**0.360**	0.231	0.373	0.262	0.398	0.292	0.423	0.317	0.448	0.320	0.449	0.328	0.457	0.436	0.534
	AVG	**0.149**	**0.289**	0.170	0.314	0.165	0.303	0.196	0.337	0.266	0.404	0.273	0.406	0.202	0.343	0.269	0.402

To further evaluate the model's performance under extreme conditions, we increased the prediction difficulty by considering scenarios where the endogenous series is extremely sparse, retaining only a single observation. As shown in Table 10, under this more challenging setting, the overall performance of all models declines. Notably, TimeSeed still achieves the best predictive performance. This can likely be attributed to our multi-stage problem decomposition strategy and reconstruction-based learning mechanism, which effectively enhance TimeSeed's generalization ability, allowing it to maintain high prediction accuracy even when available information is severely limited.

Table 10. Full results of unified hyperparameter for long-term time series forecasting results are based on a single endogenous setting, with the point selection strategy randomly sampling a time step. The look-back window length is fixed at 96. The reported results represent the average performance across different forecasting horizons $L = \{96, 192, 336, 720\}$. * indicates the use of a random sampling strategy. Lower MSE and MAE values indicate better forecasting performance.

Model		TimeSeed*		TimeSeed		DLinear*		DLinear		TimeXer*		TimeXer		FITS*		FITS	
Metric		MSE	MAE	MSE	MAE	MSE	MAE	MSE	MAE	MSE	MAE	MSE	MAE	MSE	MAE	MSE	MAE
ETTh1	96	**0.096**	**0.243**	**0.074**	**0.213**	0.104	0.262	0.078	0.221	0.402	0.529	0.314	0.469	0.131	0.291	0.100	0.251
	192	**0.113**	**0.266**	**0.098**	**0.244**	0.132	0.292	0.104	0.253	0.405	0.543	0.340	0.491	0.140	0.301	0.115	0.268
	336	**0.126**	**0.283**	**0.119**	**0.271**	0.151	0.309	0.133	0.287	0.474	0.596	0.393	0.537	0.156	0.317	0.139	0.293
	720	**0.117**	**0.272**	**0.114**	**0.267**	0.156	0.319	0.148	0.310	0.509	0.621	0.476	0.602	0.148	0.310	0.137	0.297
	AVG	**0.113**	**0.266**	**0.101**	**0.249**	0.136	0.295	0.116	0.268	0.448	0.572	0.380	0.525	0.144	0.305	0.123	0.278
ETTh2	96	**0.291**	**0.432**	**0.195**	**0.343**	0.297	0.437	0.202	0.350	0.370	0.488	0.293	0.427	0.367	0.484	0.361	0.472
	192	**0.340**	**0.471**	**0.240**	**0.386**	0.346	0.478	0.254	0.404	0.424	0.525	0.316	0.445	0.545	0.596	0.501	0.570
	336	**0.378**	**0.500**	**0.302**	**0.439**	0.393	0.509	0.308	0.444	0.425	0.526	0.358	0.479	0.788	0.732	0.603	0.635
	720	**0.398**	**0.508**	**0.339**	**0.467**	0.545	0.596	0.420	0.521	0.436	0.531	0.409	0.513	1.619	1.119	1.430	1.043
	AVG	**0.352**	**0.478**	**0.269**	**0.409**	0.395	0.505	0.296	0.430	0.414	0.518	0.344	0.466	0.830	0.733	0.723	0.680
ETTm1	96	**0.054**	**0.184**	**0.035**	**0.143**	0.054	0.184	0.039	0.151	0.331	0.500	0.314	0.492	0.054	0.183	0.035	0.144
	192	0.066	0.204	**0.051**	0.175	0.068	0.206	0.054	0.179	0.359	0.519	0.324	0.495	**0.065**	**0.200**	**0.051**	**0.172**
	336	**0.077**	**0.219**	**0.067**	**0.202**	0.081	0.226	0.071	0.207	0.370	0.520	0.317	0.478	0.077	0.220	0.067	0.203
	720	**0.097**	**0.246**	**0.091**	**0.235**	0.106	0.261	0.098	0.248	0.347	0.496	0.344	0.491	0.102	0.257	0.092	0.242
	AVG	**0.073**	**0.213**	**0.061**	**0.189**	0.077	0.219	0.065	0.196	0.352	0.509	0.325	0.489	0.074	0.215	0.061	0.190
ETTm2	96	**0.214**	**0.367**	**0.129**	**0.271**	0.222	0.371	0.150	0.290	0.271	0.409	0.216	0.348	0.258	0.397	0.212	0.360
	192	**0.237**	**0.385**	**0.159**	**0.304**	0.247	0.392	0.179	0.325	0.288	0.422	0.248	0.387	0.274	0.411	0.242	0.376
	336	**0.260**	**0.402**	**0.187**	**0.335**	0.263	0.404	0.205	0.350	0.334	0.456	0.285	0.418	0.399	0.508	0.269	0.421
	720	**0.295**	**0.434**	**0.230**	**0.376**	0.381	0.493	0.289	0.424	0.347	0.472	0.323	0.452	0.479	0.563	0.270	0.540
	AVG	**0.251**	**0.397**	**0.176**	**0.321**	0.278	0.415	0.206	0.347	0.310	0.440	0.268	0.401	0.353	0.470	0.248	0.424

G. Full Results of Ablation

To validate the effectiveness of the TimeSeed architecture, we conducted comprehensive ablation studies on all modules. The results are presented in Tables 11.

Table 11. Full results of Ablation study results on the key components of TimeSeed. PI denotes Patch-Interact (Eq. (3)), ASR denotes Adaptive Scale Reconstructor, FDA denotes Frequency Domain Aggregator, and TDA denotes Time Domain Aggregator. Moreover,, AggHigh and AggLow are defined in Eq. (7).

Model		Ours		w/o Agghigh		w/o Agglow		w/o P-I		w/o FDA		w/o TDA		w/o Sparse point		Direct Forecasting	
Metric		MSE	MAE	MSE	MAE	MSE	MAE	MSE	MAE	MSE	MAE	MSE	MAE	MSE	MAE	MSE	MAE
ETTh1	96	**0.069**	**0.203**	0.078	0.203	0.075	0.213	0.072	0.206	0.073	0.207	0.073	0.204	0.071	0.209	0.083	0.223
	192	**0.091**	**0.236**	0.098	0.236	0.098	0.245	0.097	0.238	0.097	0.238	0.095	0.234	0.095	0.240	0.122	0.268
	336	**0.111**	**0.262**	0.118	0.263	0.124	0.275	0.123	0.272	0.121	0.269	0.119	0.266	0.114	0.266	0.147	0.303
	720	**0.112**	**0.265**	0.153	0.265	0.142	0.295	0.183	0.344	0.182	0.344	0.183	0.345	0.117	0.271	0.143	0.302
	AVG	**0.096**	**0.242**	0.112	0.242	0.110	0.257	0.119	0.265	0.118	0.265	0.117	0.263	0.099	0.246	0.124	0.274
ETTm1	96	**0.036**	**0.143**	0.037	0.145	0.043	0.155	0.037	0.146	0.039	0.151	0.040	0.154	0.042	0.160	0.044	0.159
	192	**0.055**	**0.179**	0.057	0.181	0.058	0.182	0.057	0.181	0.059	0.184	0.058	0.184	0.058	0.186	0.064	0.190
	336	**0.076**	**0.210**	0.097	0.238	0.078	0.213	0.078	0.212	0.099	0.241	0.086	0.231	0.088	0.233	0.079	0.216
	720	**0.106**	**0.246**	0.146	0.297	0.127	0.272	0.125	0.268	0.154	0.311	0.148	0.308	0.142	0.296	0.110	0.253
	AVG	**0.068**	**0.194**	0.084	0.215	0.077	0.206	0.074	0.202	0.088	0.222	0.083	0.219	0.083	0.219	0.074	0.204
ETTh2	96	**0.186**	**0.336**	0.197	0.345	0.194	0.343	0.202	0.350	0.205	0.354	0.287	0.422	0.194	0.343	0.217	0.364
	192	**0.234**	**0.379**	0.237	0.380	0.260	0.397	0.259	0.399	0.270	0.410	0.336	0.461	0.239	0.386	0.287	0.423
	336	**0.288**	**0.426**	0.299	0.438	0.297	0.434	0.296	0.433	0.304	0.441	0.390	0.501	0.294	0.433	0.341	0.465
	720	**0.380**	**0.499**	0.403	0.515	0.388	0.505	0.406	0.516	0.417	0.522	0.488	0.566	0.388	0.496	0.754	0.719
	AVG	**0.272**	**0.410**	0.284	0.420	0.285	0.420	0.291	0.424	0.299	0.432	0.376	0.488	0.279	0.415	0.400	0.493
ETTm2	96	**0.092**	**0.224**	0.097	0.229	0.096	0.229	0.099	0.234	0.093	0.225	0.100	0.233	0.129	0.272	0.096	0.228
	192	**0.127**	**0.269**	0.132	0.275	0.131	0.273	0.135	0.279	0.132	0.275	0.132	0.274	0.158	0.304	0.131	0.273
	336	**0.160**	**0.304**	0.165	0.310	0.179	0.323	0.168	0.313	0.166	0.315	0.167	0.312	0.186	0.333	0.186	0.329
	720	**0.217**	**0.360**	0.224	0.367	0.229	0.371	0.220	0.363	0.223	0.357	0.219	0.362	0.231	0.377	0.228	0.371
	AVG	**0.149**	**0.289**	0.155	0.295	0.159	0.299	0.156	0.298	0.154	0.293	0.154	0.295	0.176	0.322	0.160	0.300

H. Full Results of Hard and Soft Choose

The results are presented in Tables 12.

Table 12. Full Results of Hard and Soft Choose

Model		TimeSeed		TimeSeed(Soft)	
Metric		MSE	MAE	MSE	MAE
ETTh1	96	**0.069**	**0.203**	0.075	0.211
	192	**0.091**	**0.236**	0.097	0.238
	336	**0.111**	**0.262**	0.121	0.269
	720	**0.112**	**0.265**	0.185	0.346
	AVG	**0.096**	**0.242**	0.119	0.266
ETTm1	96	**0.036**	**0.143**	0.038	0.147
	192	**0.055**	**0.179**	0.087	0.225
	336	**0.076**	**0.210**	0.077	0.211
	720	**0.106**	**0.246**	0.168	0.323
	AVG	**0.068**	**0.194**	0.092	0.226
Traffic	96	**0.421**	**0.447**	0.547	0.572
	192	**0.412**	**0.438**	0.508	0.547
	336	**0.376**	**0.417**	0.561	0.572
	720	**0.402**	**0.429**	0.563	0.579
	AVG	**0.403**	**0.433**	0.545	0.567
Weather	96	**0.002**	**0.028**	0.007	0.063
	192	**0.002**	**0.033**	0.003	0.042
	336	**0.002**	**0.035**	0.014	0.092
	720	**0.003**	**0.040**	0.013	0.088
	AVG	**0.002**	**0.034**	0.009	0.071

I. Full Results with Exogenous Variables Only

To further investigate the reconstruction capability of TimeSeed for endogenous variables, we report in Table 13 the complete prediction results obtained using only exogenous variables, without endogenous inputs. It is worth noting that a small number of models become distorted under these conditions, with prediction performance completely deteriorating, such as TimeMixer's performance on Weather. In contrast, TimeSeed models the trend and cyclical components of historical endogenous variables through decomposition, thereby enhancing robustness. Finally, it uses reconstructed historical endogenous variables to predict future changes in endogenous variables. This complex prediction problem is decomposed into several simpler subproblems for solution. As a result, it achieves satisfactory performance even under this challenging prediction setting.

Table 13. Comparison of model performance using exogenous variables only.

Model		TimeSeed		iTrans		TimeXer		TimeMixer	
Metric		MSE	MAE	MSE	MAE	MSE	MAE	MSE	MAE
Traffic	96	0.408	0.459	**0.262**	**0.332**	0.595	0.659	0.502	0.593
	192	**0.434**	**0.453**	0.798	0.740	0.601	0.662	0.581	0.648
	336	0.436	0.455	**0.386**	**0.414**	0.622	0.672	0.611	0.663
	720	**0.417**	**0.447**	1.031	0.860	0.713	0.726	0.671	0.705
	AVG	**0.424**	**0.453**	0.619	0.587	0.633	0.680	0.591	0.652
Weather	96	**0.007**	**0.069**	0.011	0.091	0.885	0.809	2.200	1.291
	192	0.007	0.069	**0.006**	**0.062**	0.754	0.732	2.363	1.370
	336	**0.007**	**0.068**	0.008	0.077	0.810	0.765	2.216	1.330
	720	**0.007**	**0.071**	0.010	0.076	0.757	0.742	2.127	1.277
	AVG	**0.007**	**0.069**	0.009	0.076	0.801	0.762	2.227	1.317

J. ERROR BARS

Here, we repeat all the experiments five times and report the standard deviation and the statistical significance test in Table 14.

Table 14. Standard deviation and statistical tests for our method.

Model	TimeSeed		Confidence
Dataset	MSE	MSE	Interval
Weather	0.002 ± 0.002	0.035 ± 0.007	0.99
ECL	0.533 ± 0.035	0.560 ± 0.019	0.99
Traffic	0.404 ± 0.017	0.435 ± 0.014	0.99
ETTh1	0.097 ± 0.003	0.243 ± 0.005	0.99
ETTh2	0.271 ± 0.004	0.409 ± 0.003	0.99
ETTm1	0.068 ± 0.003	0.194 ± 0.004	0.99
ETTm2	0.148 ± 0.002	0.289 ± 0.001	0.99

K. Full Results of Non-Overlap vs Overlap Patch

In order to better establish the mapping between the periodic components of exogenous and endogenous variables, TimeSeed employs the Patch mechanism in the Time Domain Aggregator (TDA) to more efficiently fit the periodicity that inherently exists in the dataset. Here, we report the complete results for both non-overlapping (TimeSeed) and overlapping patches (TimeSeed-OL). Based on the patch parameter settings in (Nie et al., 2022), we adopt a step size of 12 and a patch length of 24. As shown in Tables 15 and 16, the non-overlapping patch strategy (TimeSeed) and the overlapping patch strategy (TimeSeed-OL) exhibit substantial performance differences across datasets. The most pronounced disparity is observed on the ETTh1 dataset, where the performance gap reaches 61.6% in the 720-step forecasting task. Furthermore, TimeSeed consistently achieves superior average performance on ETTh1, which may be attributed to its ability to more effectively capture independent temporal features while mitigating the information redundancy introduced by overlapping regions. This conclusion is consistent with the experimental results in (Wang et al., 2024b).

Table 15. Comprehensive performance results of models using overlapping patches based on sparse endogenous variable setting (OL indicates the use of overlapping patches).

Model		TimeSeed		TimeSeed-OL	
Metric		MSE	MAE	MSE	MAE
ETTh1	96	0.069	0.203	0.075	0.211
	192	0.091	0.236	0.094	0.236
	336	0.111	0.262	0.122	0.271
	720	0.112	0.265	0.181	0.342
	AVG	0.096	0.242	0.118	0.265
ETTh2	96	0.186	0.336	0.191	0.341
	192	0.234	0.379	0.232	0.378
	336	0.288	0.426	0.287	0.425
	720	0.380	0.499	0.386	0.504
	AVG	0.272	0.410	0.274	0.412
ETTm1	96	0.036	0.143	0.037	0.146
	192	0.055	0.179	0.06	0.185
	336	0.076	0.210	0.077	0.211
	720	0.106	0.246	0.105	0.244
	AVG	0.068	0.194	0.07	0.197
ETTm2	96	0.092	0.224	0.094	0.226
	192	0.127	0.269	0.128	0.27
	336	0.160	0.304	0.161	0.306
	720	0.217	0.360	0.213	0.356
	AVG	0.149	0.289	0.149	0.29
Traffic	96	0.421	0.447	0.422	0.446
	192	0.412	0.438	0.423	0.447
	336	0.376	0.417	0.407	0.44
	720	0.402	0.429	0.383	0.417
	AVG	0.403	0.433	0.409	0.437
ECL	96	0.516	0.555	0.512	0.554
	192	0.514	0.550	0.508	0.546
	336	0.510	0.542	0.539	0.563
	720	0.576	0.586	0.572	0.584
	AVG	0.529	0.558	0.532	0.562

Table 16. Comprehensive performance results of models using overlapping patches based on a single endogenous variable setting (OL indicates the use of overlapping patches).

Model		TimeSeed		TimeSeed-OL	
Metric		MSE	MAE	MSE	MAE
ETTh1	96	0.074	0.213	0.070	0.209
	192	0.098	0.244	0.093	0.238
	336	0.119	0.271	0.117	0.270
	720	0.114	0.267	0.114	0.267
	AVG	0.101	0.249	0.099	0.246
ETTh2	96	0.195	0.343	0.190	0.340
	192	0.240	0.386	0.238	0.386
	336	0.302	0.439	0.299	0.437
	720	0.339	0.467	0.328	0.460
	AVG	0.269	0.409	0.264	0.406
ETTm1	96	0.035	0.143	0.036	0.146
	192	0.051	0.175	0.053	0.179
	336	0.067	0.202	0.068	0.204
	720	0.091	0.235	0.092	0.236
	AVG	0.061	0.189	0.062	0.191
ETTm2	96	0.129	0.271	0.129	0.271
	192	0.159	0.304	0.159	0.305
	336	0.187	0.335	0.188	0.334
	720	0.230	0.376	0.230	0.375
	AVG	0.176	0.321	0.177	0.322
ECL	96	0.515	0.560	0.511	0.550
	192	0.518	0.550	0.611	0.602
	336	0.595	0.588	0.621	0.606
	720	0.648	0.621	0.621	0.611
	AVG	0.569	0.580	0.591	0.592
Traffic	96	0.489	0.492	0.464	0.481
	192	0.482	0.484	0.477	0.489
	336	0.496	0.503	0.489	0.493
	720	0.459	0.477	0.490	0.495
	AVG	0.482	0.489	0.480	0.489

L. Case Study

To further evaluate our proposed model, we report complementary predictive visualization results on the ETT dataset. For baseline selection, we select representative models, including FITS (Xu et al., 2023), PatchTST (Nie et al., 2022), and DLinear (Zeng et al., 2023). As shown in Figures 15 and 16, TimeSeed performs best in fitting the ground truth, demonstrating excellent predictive performance.

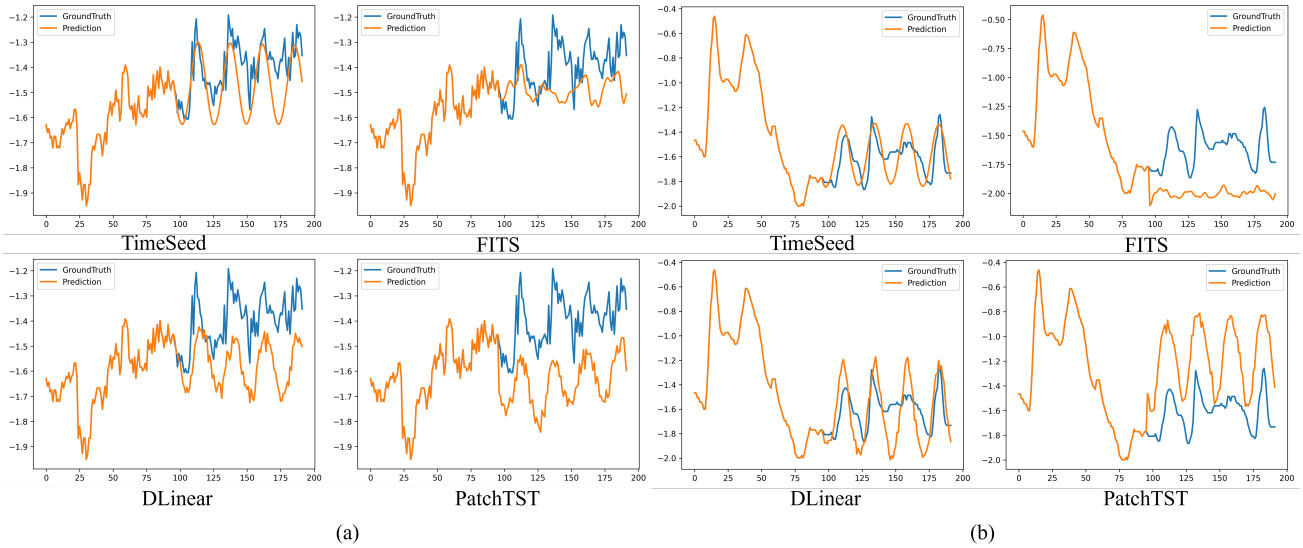

Figure 15. Prediction cases from TimeSeed, FITS, DLinear, and PatchTST on the ETTh1 (a) and ETTh2 (b) datasets under the input-96-predict-96 setting. Blue lines are the ground truths and orange lines are the model predictions.

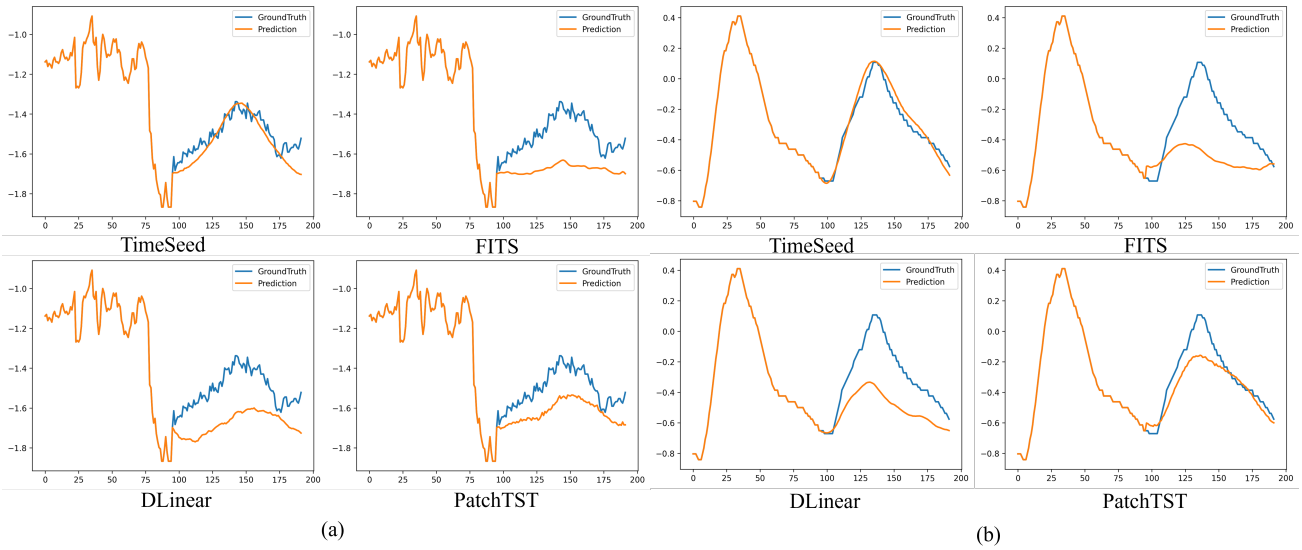

Figure 16. Prediction cases from TimeSeed, FITS, DLinear, and PatchTST on the ETTm1 (a) and ETTm2 (b) datasets under the input-96-predict-96 setting. Blue lines are the ground truths and orange lines are the model predictions.

M. Full Main Results

We report the results of long time series prediction based on sparse endogenous settings (with missing observations) and one single endogenous settings (without exogenous variables), with prediction lengths including {96, 192, 336, 720}, where the size of the look back window is fixed to 96. All experiments are performed with the unified hyperparameter settings as described earlier. As shown in Tables 17 and 18, TimeSeed achieves optimal performance on almost all metrics compared with baseline models. Notably, under the sparse and single endogenous settings, TimeSeed attains the highest ranking across 59 and 62 evaluation cases (1st Count), respectively, which is substantially more frequent than any baseline model.

Table 17. Full results of unified hyperparameter for long-term time series forecasting results are based on sparse endogenous setting, with the point selection strategy choosing the most recent time step. The look-back window length is fixed at 96. Lower MSE and MAE values indicate better forecasting performance. The best results are highlighted in red, and the second-best results are highlighted in blue.

Model		TimeSeed		DUET		iTrans		DLinear		TimeXer		TimeMixer		PatchTST		FITS		CycleNet		TexFilter		PaiFilter		SparseTSF	
Metric		MSE	MAE	MSE	MAE	MSE	MAE	MSE	MAE	MSE	MAE	MSE	MAE	MSE	MAE	MSE	MAE	MSE	MAE	MSE	MAE	MSE	MAE	MSE	MAE
ETTh1	96	**0.069**	**0.203**	0.124	0.276	0.170	0.334	0.079	0.218	0.438	0.572	0.102	0.243	0.106	0.259	0.089	0.230	0.078	0.212	0.100	0.245	0.079	0.222	0.123	0.277
	192	**0.091**	**0.236**	0.123	0.268	0.157	0.316	0.105	0.251	0.442	0.565	0.109	0.253	0.320	0.467	0.211	0.372	0.097	0.237	0.108	0.254	0.155	0.309	0.156	0.315
	336	0.111	0.262	0.180	0.336	0.248	0.403	0.138	0.292	0.429	0.552	0.267	0.413	0.205	0.356	0.120	0.273	**0.109**	**0.255**	0.133	0.287	0.242	0.402	0.178	0.338
	720	**0.112**	**0.265**	0.210	0.364	0.168	0.326	0.131	0.288	0.464	0.588	0.170	0.328	0.281	0.442	0.149	0.311	0.180	0.340	0.235	0.389	0.133	0.290	0.175	0.334
	AVG	**0.096**	**0.242**	0.159	0.311	0.186	0.345	0.113	0.262	0.444	0.569	0.162	0.309	0.228	0.381	0.142	0.297	0.116	0.261	0.144	0.294	0.152	0.306	0.158	0.316
ETTh2	96	**0.186**	**0.336**	0.363	0.475	0.581	0.655	0.201	0.350	0.289	0.423	0.213	0.355	0.436	0.535	0.303	0.431	0.198	0.345	0.368	0.482	0.251	0.395	0.377	0.490
	192	**0.234**	**0.379**	0.334	0.461	1.071	0.890	0.255	0.397	0.330	0.457	0.255	0.393	1.017	0.887	0.333	0.460	0.243	0.387	0.314	0.446	0.321	0.453	0.477	0.555
	336	0.288	0.426	0.423	0.512	0.922	0.825	0.306	0.440	0.358	0.479	0.299	0.438	0.458	0.552	0.496	0.571	0.309	0.441	**0.283**	**0.423**	0.413	0.517	0.607	0.637
	720	0.380	0.499	0.406	0.517	1.034	0.873	0.873	0.786	0.390	0.501	**0.331**	**0.462**	0.384	0.494	1.079	0.887	0.414	0.519	0.347	0.473	0.915	0.815	1.028	0.859
	AVG	**0.272**	**0.410**	0.381	0.491	0.902	0.811	0.409	0.493	0.342	0.465	0.274	0.412	0.574	0.617	0.553	0.587	0.291	0.423	0.328	0.456	0.475	0.545	0.622	0.635
ETTm1	96	**0.036**	**0.143**	0.068	0.202	0.046	0.164	0.043	0.157	0.290	0.468	0.107	0.274	0.046	0.166	0.051	0.175	0.044	0.158	0.114	0.266	0.050	0.172	0.046	0.164
	192	**0.055**	**0.179**	0.094	0.237	0.074	0.209	0.064	0.191	0.301	0.468	0.137	0.306	0.068	0.196	0.083	0.226	0.094	0.241	0.055	0.180	0.069	0.205	0.065	0.196
	336	**0.076**	**0.210**	0.200	0.363	0.357	0.524	0.083	0.218	0.359	0.508	0.152	0.306	0.123	0.275	0.092	0.231	0.126	0.280	0.225	0.388	0.194	0.362	0.086	0.227
	720	0.106	0.246	0.265	0.409	0.095	**0.232**	0.111	0.253	0.426	0.551	0.170	0.336	0.181	0.341	**0.088**	0.232	0.153	0.306	0.186	0.343	0.123	0.279	1.800	1.277
	AVG	**0.068**	**0.194**	0.157	0.303	0.143	0.282	0.075	0.205	0.344	0.499	0.141	0.305	0.104	0.245	0.079	0.216	0.104	0.246	0.145	0.294	0.109	0.254	0.499	0.466
ETTm2	96	**0.092**	**0.224**	0.247	0.392	0.140	0.294	0.093	0.224	0.239	0.377	0.103	0.248	0.197	0.368	0.118	0.260	0.096	0.226	0.119	0.259	0.106	0.243	0.127	0.273
	192	**0.127**	**0.269**	0.225	0.365	0.399	0.543	0.135	0.276	0.245	0.384	0.177	0.330	0.225	0.384	0.151	0.298	0.133	0.273	0.151	0.297	0.168	0.317	0.164	0.315
	336	**0.160**	**0.304**	0.313	0.443	0.381	0.517	0.171	0.315	0.261	0.404	0.160	0.310	0.188	0.333	0.212	0.357	0.171	0.315	0.178	0.324	0.200	0.345	0.201	0.350
	720	**0.217**	**0.360**	0.350	0.471	0.573	0.627	0.262	0.398	0.317	0.448	0.276	0.411	0.224	0.365	0.328	0.457	0.230	0.371	0.257	0.394	0.231	0.376	0.279	0.418
	AVG	**0.149**	**0.289**	0.284	0.417	0.373	0.495	0.165	0.303	0.266	0.404	0.179	0.325	0.208	0.362	0.202	0.343	0.157	0.296	0.176	0.318	0.176	0.320	0.193	0.339
Weather	96	**0.002**	**0.028**	0.007	0.059	0.009	0.078	0.014	0.081	0.758	0.751	0.005	0.063	0.003	0.041	0.005	0.060	0.004	0.043	0.003	0.038	0.005	0.050	0.005	0.059
	192	**0.002**	**0.033**	0.005	0.054	0.020	0.109	0.003	0.045	0.831	0.793	0.468	0.680	0.006	0.059	0.009	0.072	0.003	0.039	0.007	0.061	0.008	0.070	0.008	0.077
	336	**0.002**	**0.035**	0.005	0.060	0.005	0.058	0.008	0.066	0.814	0.782	0.409	0.636	0.005	0.054	0.008	0.072	0.002	0.035	0.004	0.049	0.005	0.053	0.008	0.073
	720	**0.003**	**0.040**	0.006	0.058	0.008	0.076	0.009	0.074	0.905	0.831	0.692	0.828	0.004	0.046	0.006	0.062	0.003	0.040	0.006	0.060	0.030	0.134	0.006	0.064
	AVG	**0.002**	**0.034**	0.006	0.058	0.011	0.080	0.009	0.066	0.827	0.789	0.394	0.552	0.004	0.050	0.007	0.067	0.003	0.039	0.005	0.052	0.012	0.077	0.007	0.068
ECL	96	**0.516**	**0.555**	0.605	0.606	1.047	0.820	0.800	0.684	0.558	0.563	1.869	1.060	0.776	0.683	1.499	1.007	0.784	0.675	0.811	0.700	0.983	0.787	0.712	0.655
	192	**0.514**	0.550	0.579	0.582	0.693	0.666	0.824	0.695	0.533	**0.549**	2.369	1.239	0.624	0.620	1.329	0.912	0.780	0.669	0.724	0.640	1.043	0.823	0.764	0.684
	336	**0.510**	**0.542**	0.665	0.629	0.603	0.595	0.710	0.642	0.571	0.569	1.978	1.120	0.605	0.592	0.696	0.640	0.850	0.701	0.911	0.737	0.817	0.698	0.641	0.624
	720	0.576	0.586	0.713	0.654	0.652	0.624	0.994	0.776	0.638	0.611	**0.480**	**0.526**	0.851	0.741	0.822	0.707	0.872	0.715	0.655	0.630	1.267	0.927	0.717	0.662
	AVG	**0.529**	**0.558**	0.641	0.618	0.749	0.676	0.832	0.699	0.575	0.573	1.674	0.987	0.714	0.659	1.087	0.817	0.822	0.690	0.775	0.677	1.027	0.809	0.709	0.656
Traffic	96	**0.421**	**0.447**	0.668	0.621	0.441	0.457	0.569	0.537	1.345	1.012	0.635	0.603	0.531	0.527	0.629	0.595	0.885	0.684	0.583	0.552	0.473	0.475	1.236	0.876
	192	**0.412**	**0.438**	0.543	0.538	0.646	0.607	0.485	0.481	1.436	1.056	1.363	0.874	0.516	0.516	0.653	0.609	0.875	0.676	0.683	0.597	0.946	0.764	1.220	0.859
	336	**0.376**	**0.417**	0.571	0.570	0.425	0.458	0.671	0.590	1.363	0.995	1.627	0.951	0.431	0.474	0.909	0.722	0.875	0.678	0.476	0.491	0.461	0.485	1.287	0.896
	720	**0.402**	**0.429**	0.515	0.515	0.419	0.452	0.611	0.558	1.441	1.047	1.379	0.885	0.518	0.519	0.970	0.764	0.869	0.672	0.594	0.554	0.932	0.750	1.361	0.913
	AVG	**0.403**	**0.433**	0.574	0.561	0.483	0.493	0.584	0.542	1.396	1.028	1.251	0.828	0.499	0.509	0.790	0.672	0.876	0.678	0.584	0.548	0.703	0.619	1.276	0.886
1st Count		**30**	**29**	0	0	0	1	0	0	0	1	2	2	0	0	1	0	1	1	1	1	0	0	0	0

Table 18. Full results of unified hyperparameter for long-term time series forecasting results are based on a single endogenous setting, with the point selection strategy choosing the most recent time step. The look-back window length is fixed at 96. Lower MSE and MAE values indicate better forecasting performance. The best results are highlighted in red, and the second-best results are highlighted in blue.

Model	Metric	TimeSeed		DUET		iTrans		DLinear		TimeXer		TimeMixer		PatchTST		FITS		CycleNet		TexFilter		PaiFilter		SparseTSF	
		MSE	MAE	MSE	MAE	MSE	MAE	MSE	MAE	MSE	MAE	MSE	MAE	MSE	MAE	MSE	MAE	MSE	MAE	MSE	MAE	MSE	MAE	MSE	MAE
ETTh1	96	**0.074**	**0.213**	0.108	0.259	0.172	0.332	0.078	0.221	0.314	0.469	0.441	0.582	0.105	0.257	0.100	0.251	0.284	0.444	0.083	0.230	0.079	0.221	0.137	0.295
	192	**0.098**	**0.244**	0.124	0.276	0.151	0.308	0.104	0.253	0.340	0.491	0.470	0.579	0.201	0.365	0.115	0.268	0.327	0.475	0.110	0.259	0.142	0.297	0.165	0.328
	336	**0.119**	**0.271**	0.169	0.323	0.203	0.348	0.133	0.287	0.393	0.537	0.793	0.789	0.159	0.304	0.139	0.293	0.332	0.485	0.133	0.288	0.132	0.284	0.188	0.348
	720	**0.114**	**0.267**	0.357	0.472	0.189	0.342	0.148	0.310	0.476	0.602	0.448	0.578	0.205	0.359	0.137	0.297	0.431	0.564	0.175	0.327	0.134	0.291	0.181	0.340
	AVG	**0.101**	**0.249**	0.189	0.332	0.179	0.332	0.116	0.268	0.380	0.525	0.538	0.632	0.168	0.321	0.123	0.278	0.343	0.492	0.125	0.276	0.121	0.273	0.168	0.328
ETTh2	96	**0.195**	**0.343**	0.318	0.440	0.560	0.637	0.202	0.350	0.293	0.427	0.403	0.492	0.547	0.605	0.361	0.472	0.285	0.420	0.653	0.651	0.239	0.386	0.384	0.493
	192	**0.240**	**0.386**	0.362	0.481	1.228	0.980	0.254	0.404	0.316	0.445	0.536	0.568	0.920	0.827	0.501	0.570	0.312	0.445	0.313	0.444	0.275	0.420	0.498	0.567
	336	**0.302**	**0.439**	0.356	0.474	0.788	0.755	0.308	0.444	0.358	0.479	0.562	0.592	0.419	0.530	0.603	0.635	0.366	0.484	0.307	0.443	0.452	0.544	0.641	0.657
	720	0.339	0.467	0.432	0.528	1.071	0.891	0.420	0.521	0.409	0.513	0.661	0.652	0.598	0.629	1.430	1.043	0.410	0.513	**0.328**	**0.458**	0.883	0.797	1.179	0.926
	AVG	**0.269**	**0.409**	0.367	0.481	0.912	0.816	0.296	0.430	0.344	0.466	0.540	0.576	0.621	0.648	0.723	0.680	0.343	0.465	0.400	0.499	0.462	0.537	0.676	0.661
ETTm1	96	**0.035**	**0.143**	0.049	0.170	0.060	0.187	0.039	0.151	0.314	0.492	0.625	0.655	0.053	0.176	**0.035**	0.144	0.204	0.381	0.044	0.159	0.040	0.152	0.049	0.170
	192	**0.051**	0.175	0.077	0.214	0.074	0.211	0.054	0.179	0.324	0.495	0.476	0.559	0.059	0.190	**0.051**	**0.172**	0.224	0.396	0.054	0.178	0.074	0.211	0.073	0.211
	336	**0.067**	**0.202**	0.102	0.249	0.100	0.244	0.071	0.207	0.317	0.478	0.458	0.542	0.106	0.254	**0.067**	0.203	0.237	0.399	0.095	0.242	0.106	0.257	0.099	0.247
	720	**0.091**	**0.235**	0.154	0.313	0.099	0.249	0.098	0.248	0.344	0.491	0.394	0.507	0.101	0.253	0.092	0.242	0.267	0.422	0.099	0.246	0.112	0.267	0.139	0.297
	AVG	**0.061**	**0.189**	0.096	0.237	0.083	0.223	0.065	0.196	0.325	0.489	0.488	0.566	0.080	0.218	**0.061**	0.190	0.233	0.400	0.073	0.206	0.083	0.222	0.090	0.231
ETTm2	96	**0.129**	**0.271**	0.317	0.449	0.151	0.292	0.150	0.290	0.216	0.348	0.168	0.311	0.144	0.286	0.212	0.360	0.233	0.370	0.244	0.377	0.192	0.344	0.224	0.373
	192	**0.159**	**0.304**	0.215	0.358	0.383	0.527	0.179	0.325	0.248	0.387	0.223	0.366	0.170	0.319	0.242	0.376	0.262	0.399	0.172	0.314	0.261	0.399	0.233	0.379
	336	**0.187**	**0.335**	0.280	0.417	0.304	0.441	0.205	0.350	0.285	0.418	0.252	0.393	0.230	0.374	0.269	0.421	0.301	0.429	0.189	0.336	0.214	0.362	0.248	0.392
	720	**0.230**	**0.376**	0.321	0.443	0.544	0.613	0.289	0.424	0.323	0.452	0.314	0.439	0.254	0.401	0.270	0.540	0.336	0.463	0.259	0.397	0.258	0.402	0.292	0.426
	AVG	**0.176**	**0.321**	0.283	0.417	0.345	0.468	0.206	0.347	0.268	0.401	0.239	0.377	0.200	0.345	0.248	0.424	0.283	0.415	0.216	0.356	0.231	0.377	0.249	0.392
ECL	96	**0.515**	**0.560**	0.822	0.712	1.185	0.892	1.018	0.773	0.570	0.570	0.609	0.605	0.752	0.666	1.711	1.061	0.698	0.636	0.729	0.652	0.821	0.706	0.941	0.763
	192	**0.518**	**0.550**	0.741	0.687	0.687	0.649	0.923	0.739	0.580	0.573	0.707	0.651	0.801	0.686	1.141	0.830	0.725	0.645	0.953	0.748	0.779	0.680	0.994	0.779
	336	**0.595**	**0.588**	0.622	0.600	0.647	0.611	0.724	0.644	0.609	0.591	0.674	0.630	0.758	0.673	0.680	0.631	0.748	0.654	0.856	0.711	0.862	0.719	0.781	0.686
	720	**0.648**	**0.621**	0.675	0.636	0.833	0.712	1.666	1.041	0.718	0.644	0.658	0.627	0.943	0.781	0.866	0.727	0.818	0.695	0.872	0.719	0.788	0.690	0.829	0.707
	AVG	**0.569**	**0.580**	0.715	0.659	0.838	0.716	1.083	0.799	0.619	0.594	0.662	0.628	0.813	0.701	1.099	0.812	0.747	0.657	0.853	0.708	0.813	0.699	0.886	0.734
Traffic	96	0.489	0.492	0.663	0.609	0.490	0.491	**0.479**	**0.490**	1.514	1.081	1.334	1.008	0.490	0.493	0.784	0.674	1.436	1.030	0.803	0.667	1.377	0.964	1.532	0.972
	192	**0.482**	**0.484**	0.547	0.549	0.644	0.612	0.596	0.551	1.578	1.064	1.440	1.061	0.495	0.507	0.967	0.771	1.548	1.079	0.681	0.603	0.817	0.714	1.592	0.986
	336	0.496	0.503	0.526	0.541	**0.410**	**0.443**	0.626	0.566	1.499	1.056	1.393	1.040	0.453	0.491	0.936	0.748	1.559	1.093	0.937	0.733	1.038	0.812	1.457	0.944
	720	**0.459**	**0.477**	0.605	0.580	0.477	0.483	0.708	0.605	1.606	1.112	1.452	1.056	0.470	0.503	0.977	0.773	1.678	1.131	0.630	0.582	0.875	0.732	1.806	1.059
	AVG	0.482	**0.489**	0.585	0.570	0.505	0.507	0.602	0.553	1.549	1.078	1.405	1.041	**0.477**	0.498	0.916	0.741	1.555	1.083	0.763	0.646	1.027	0.805	1.597	0.990
Weather	96	**0.002**	**0.028**	0.009	0.075	0.007	0.065	0.014	0.087	0.815	0.778	2.336	1.354	0.003	0.041	0.003	0.043	0.909	0.829	0.005	0.058	0.005	0.052	0.006	0.062
	192	**0.002**	**0.032**	0.004	0.046	0.007	0.064	0.004	0.049	0.738	0.733	2.137	1.295	0.004	0.051	0.008	0.071	0.783	0.760	0.004	0.048	0.008	0.070	0.004	0.050
	336	**0.002**	**0.035**	0.004	0.053	0.013	0.092	0.011	0.086	0.731	0.730	3.159	1.575	0.004	0.048	0.011	0.084	0.850	0.798	0.006	0.061	0.005	0.058	0.006	0.065
	720	**0.003**	**0.040**	0.006	0.062	0.008	0.073	0.008	0.073	0.684	0.707	2.475	1.398	0.004	0.051	0.006	0.060	0.790	0.767	0.005	0.056	0.029	0.132	0.005	0.058
	AVG	**0.002**	**0.034**	0.006	0.059	0.009	0.073	0.009	0.074	0.742	0.737	2.527	1.406	0.004	0.048	0.007	0.065	0.833	0.789	0.005	0.056	0.012	0.078	0.005	0.059
1st Count		**31**	**31**	0	0	1	1	1	1	0	0	0	0	1	0	4	1	0	0	1	1	0	0	0	0